JPRS-CST-93-017
21 October 1993

JPRS Report

Science & Technology

China

Science & Technology
China

JPRS-CST-93-017 21 October 1993

CONTENTS

TELECOMMUNICATIONS R&D

TAIWAN

State To Promote Privately Owned S&T Enterprises

93FE0824A Beijing RENMIN RIBAO OVERSEAS EDITION in Chinese 25 Jun 93 p 3

[Article by reporters Yang Zhaobo [2799 0340 3134] and Yang Ning [2799 1380]]

[Text] In order to advance the development of privately operated S&T enterprises in China, promote economies of scale in privately operated S&T enterprises, and raise the level of technology and internal management, the State S&T Commission and the State Commission for Restructuring the Economy issued the "Decision on Certain questions Concerning Major Development of Privately Operated S&T Enterprises." The "Decision" systematically summarizes the experiences of privately operated Chinese S&T enterprises, and proposes guidance and relevant policies for advancing privately operated S&T enterprises. It is the first policy document on aspects of encouraging and guiding privately operated enterprises since the launching of national reforms.

The State S&T Commission and the State Commission for Restructuring the Economy held a news conference on 25 June to give a detailed description of the privately operated Chinese enterprise situation. It was learned that the origin of privately run S&T enterprises in China could be traced back to the early 80s. In March of 1985, "The CPC Central Committee Decision on Organizational Reform in Science and Technology" set the policy of "permitting collective and individually established scientific research and technological service organizations," and, thereafter, privately operated S&T organizations developed rapidly. Today, there are over 30,000 privately operated S&T enterprises, including those mainly set up by scientists and technicians, those operated collectively, cooperatively, by joint stock, or singularly, and privately run S&T organizations that are personally managed economically, together with State S&T academies and institutes, special schools and colleges, and state-owned privately operated enterprises that are set up as large and middle-sized enterprises, of which, according to 1992 statistics, more than 2,600 are privately run S&T organizations that employ nearly 400,000 persons, in technology, industry, and trade, earning 12.4 billion yuan, covering every conceivable kind of business in the economy, and adding on to that the state-owned privately operated national enterprises, they make up a fair proportion, in number and scale, of China's forerunner S&T enterprises.

"The Decision" passed down from the State S&T Commission and State Commission for Restructuring the Economy, proposes to continue the new historical period of new ideas and new points of view to promote and guide the various privately operated S&T enterprises onto faster and better development; encourages national S&T enterprises to convert their management systems, explore forms of privately operated national S&T enterprises, guide town and village enterprises in taking advantage of private ownership, get on track with scientific advances, solidify and develop joint and mutually supportive structures between national state-operated S&T enterprises and various types of privately operated S&T enterprises, to form new national, collective, and individually operated S&T industries.

The decision asserted that privately owned S&T enterprises are the product of national S&T and economic system reforms, actively created by technicians who are liberating and opening up the first power of production. Over 10 years of experience has shown that privately owned S&T enterprises are a vital force for the development of China's scientific activities and high-tech industries, and they are constituent elements of socialism. The important functions of privately owned S&T enterprises in China's reform and development are: in creating a new dynamic enterprise mechanism of "raising their own funds, making voluntary associations, self-management, and being responsible for their own profits and losses"; pragmatically using the market as their guide, synthesizing technology, industry, and trade, a new technologically molded system of production, supply, and sales; changing the long-standing system of a singular state-operated country into one based mainly on public ownership with many mutually supportive economic parts working in common for a new makeup.

"The Decision" states that in developing Chinese privately owned S&T enterprises the policy of public ownership is paramount and coexistence of multiple economic elements will be consistently supported. Every kind of privately operated S&T enterprise will be a fully functioning corporate enterprise or economic entity with clear property rights, and organizational and operational integrity in the socialist market economy. In the process of adjusting the structure of the S&T system, and distributing talent, even more scientists and technicians must be mobilized to go out into the society to set up privately operated S&T enterprises. State-owned S&T organizations, high level schools and colleges, large and middle-sized enterprises must be encouraged to set up new S&T enterprises on the state-owned privately operated model. Every sort of privately managed S&T enterprise should be developed through myriad ways and levels in accordance with industrial policy and the needs of the market.

"The Decision" declares that, hereafter, newly created privately operated S&T enterprises will be founded on definitive property rights in a standardized enterprise system according to pertinent laws and regulations. According to their makeup, privately managed S&T enterprises may execute contracts, leases, trusts, commissions, associations, and many such special forms of management. Whatever their form, they must guarantee the employee's democratic rights to function in management, financial health, accounting, labor merits, social insurance, internal assignments, and project management.

"The Decision" fully affirms the status and function of privately operated S&T enterprises, changes the singular restrictive policy of the past for enterprise management, and realistically sets the conditions for long-term coexistence, common development, and equal competition for the various kinds of privately managed S&T enterprises. Previously established policies will be eliminated according to the requirements for creating a socialist market-economy system, and continue to enrich and perfect all measures that benefit the development of privately operated S&T enterprises. Those measures detrimental to the market economic system and not conducive to the development of privately operated S&T enterprises should

be revised, augmented, or rescinded procedurally in proper time. To further invigorate privately operated S&T enterprises, their independent authority to make investment policy decisions, manage, engage in research, production and sales, to set prices for products, and to make internal assignments and professional evaluations will be guaranteed, and they will be actively supported and guided in their efforts to constantly improve technology and form new mechanisms. Their legal rights and interests must be guaranteed according to the law. Basically, the principle of individual equality before the law will apply to the handling of technical and economic disputes involving privately operated S&T enterprises. All levels of government and their relevant departments must be on the forefront of reforms, and must realistically strengthen their leadership and close cooperation, integrate the special characteristics of local S&T, talent, and resources, and formulate plans for the development of privately operated S&T enterprises. They must improve pertinent policies and measures, promptly study and resolve new situations and new issues that arise out of reform and development, and comprehensively apply economic, policy, and legal measures to push the specialized privately operated S&T industries on to greater heights, greater scope, and greater profits.

$150 Million Invested in Building High-Tech Base in Jinqiao

93FE0824B Shanghai WEN HUI BAO in Chinese
5 May 93 p 1

[Article by correspondent Gui Huakuang [2710 5478 0400] and reporter Zhu Hongcai [2712 1347 4965]]

[Text] Up to the present, China's key major colleges and research units have invested over US$150 million in the Jinqiao Development Zone, to build a base for an S&T city and a line of high-tech industries. On 4 May, the Municipal Science and Technology Commission chairman, Hua Yuda [5478 5940 6671], led a group of over 50 leaders of scientific institutes to Jinqiao to discuss the establishment of an applied research zone. The CAS Shanghai Branch Academy signed an agreement with Jinqiao to invest nearly 100 million yuan to build an S&T activities building. The Jinqiao Development Zone has received investments amounting to over US$200 million, including the investments by major colleges and research units for 12 projects. The major colleges that invested in Jinqiao set up the China Major Colleges Group Corporation composed of 33 key major colleges of the State Education Committee, and in addition to investing nearly 100 million for the building, on 4 May they also decided to invest 30 million yuan to build a scientific research industrial base to assist the university investment projects.

A group of China's best research units and the S&T Industrial Corporation were also actively investing in Jinqiao to make this export-processing zone into a center for Shanghai's high-tech industrialization. The CAS Shanghai Branch Academy set up the Shanghai Mutual S&T Development Corporation at Jinqiao joining the Shanghai Technical Physics Institute and the Silicate Research Institute in an effort to develop bio-technology, new materials science, opto-electronics and laser technology. The China Huitong Group Corporation, China Jupu Group Corporation, and the Northern Opto-Electronics New Technology Research Institute have combined forces at Jinqiao to produce copying facilities, electronic communications, computer networks, human ecological control and adjustment systems, hydropower, and electric power distribution systems, precision opto-electronic surveying instruments, and hydraulic automobile transmissions.

It was learned that activity and construction has already begun on a group of structures to be built at Jinqiao with an investment of over 500 million yuan from the major colleges, research units and S&T corporations, for the S&T city, covering an area of 150,000 square meters. The majority of buildings will be built on the No. 15 block in the Jinqiao Development Zone.

Beijing Simulation Center Profiled

93FE0954A Beijing LIAOWANG ZHOUKAN [LIAOWANG WEEKLY] in Chinese
No 33, 16 Aug 93 pp 4-5

[Article by Li Li [2621 2980]: "Chinese Simulation Technology Among Leaders Worldwide"]

[Text] After 8 years of development, innovation and importation, the Beijing Simulation Center, the largest and most technically advanced center in Asia, has finally been established at the Second Research Institute of the Aerospace Industry Corporation. On 30 July, Song Jian [1345 0256], a member of the State Council and chairman of the State Science and Technology Commission, cut its ribbon as a part of the official governmental inspection ceremony. The Beijing Simulation Center is rated at world class level and contains a number of innovative features. It is praised as the "pearl of simulation." This is an announcement to the world that China is among the leaders in simulation technology.

Since it was listed as a key project in the Seventh 5-Year Plan by the State Planning Commission and the State Commission of Science, Technology and Industry for National Defense, the Beijing Simulation Center followed the rule that put the facilities to use as construction progressed in order to obtain results as early as possible. It has completed the simulation of a number of models. This not only ensured the success of large-scale flight tests but also effectively reduced the number of tests, shortened the development cycle and created obvious economic benefits. It has already made substantial contribution to aerospace technology in China. According to a scientific expert, this is another major technological accomplishment following the Beijing Electron Position Collider and the 1 billion operations per second Galaxy-IIsupercomputer. Chairman Jiang Zemin [3068 3419 3046] and Premier Li Peng [2621 7720] respectively issued the following encouragement to the Beijing Simulation Center, "Development simulation technology in China to reach the peak of high technology" and "Develop system simulation to contribute to the modernization of science and technology."

A Technology of the Right Time

Simulation is a rising leading-edge technology in advanced countries. It is a new discipline that is built on the basis of control theory, similarity principle and computer technology. With the aid of a model of a real (or imaginary)

system, a series of experiments can be performed on the system. In simple terms, it is a technology to obtain equivalent experimental results of a real event by means of modeling in a laboratory.

For instance, in the development of a new generation of spacecraft or carrier rocket it is not feasible and economically affordable to carry out repeated tests of the real object. It will have to rely on simulation. It can be simulated thousands of times in the laboratory before conducting an experiment on an actual object. It is not only safe and reliable, but also cost effective.

As another example, to develop countermeasures in the event of a nuclear accident in a power plant, it is not possible to react to an accident after it occurs. It is only possible to practice in a laboratory using simulation in order to develop various emergency procedures corresponding to different situations.

According to statistics available abroad, simulation can reduce the real time practice by 40 to 60 percent and shorten the development time by 30 to 40 percent. Moreover, it is safe, economical, controllable, non-destructive and repeatable. This is why simulation has received a great deal of attention and is becoming a highly complex system. It is an indispensable tool for research, design, evaluation and training in high-tech industries.

According to experts, simulation technology was first developed for military applications. It can be used in the development of every important weapons system, in the training of operators of any military equipment and weapons systems, in the coalition drill involving all branches of the military and in battlefield management. As military technology advances at a high speed, simulation is becoming more important and is moving to a higher level. It has gone beyond the military domain and is penetrating into a variety of fields. It is becoming a new high-tech industry.

In the past decade, a number of countries, especially developed nations, are giving priority to the development of this technology. Since 1989, simulation was listed as a high priority item in the "defense-related key technology plan" prepared by the U.S. Department of Defense. In 1992, the Pentagon realigned its technology strategic plan to prioritize seven technical fields. "Training and simulation" is one of such fields. Simulation technology was even viewed as a major driving force for future technology development by the Pentagon. Simulation was also included as one of 11 top priority technical cooperation items in the Euclid plan by the NATO countries in 1989. According to experts' prediction, these countries will still focus their investment on space technology and simulation in the next 10 to 15 years.

This "simulation rush" brings about a serious subject to China's attention in the midst of reform. In order to have a role in world politics and economy in the 21st century, China must develop simulation technology.

Results of Independent Effort

Simulation in China could be traced back to the simple simulators developed in the 60's. However, it was very primitive. By the late 70's and early 80's, there was a more urgent demand for simulation. The Ministry of Aerospace Industry also began to realize the importance of this project and started some internal preparation work. In 1982-1983, the concept of building a large-scale, technologically advanced simulation center was proposed. Was this type of rare project feasible in China? This question was carefully and scientifically evaluated. Finally, the leadership at the Ministry of Aeronautics and Astronautics Industry unanimously endorsed this idea. In 1984, a policy with creative spirit was made official.

Leaders in the Ministry of Aerospace Industry decided to employ a large-system method to manage the construction of the simulation center. It established an administrative chain of command and a technical chain of command. It named Research Fellow Xu Naiming [1776 0035 2494] as the project manager and chief commander, Research Fellow Fang Huihuang [2455 6540 3552] as the chief designer and Jiang Cuoping [5592 6783 1627] as the director of the preparation office who played a pivotal role as the overall coordinator of the project. Xu Naiming, a graduate of the class of 1951 from the Department of Mechanical Engineering of Qinghua University, is an expert in flight vehicles and an experienced aerospace engineer. He has participated in numerous key rocket development projects and for a time was the chief commander of several projects simultaneously. Fang Huihuang is a system engineering expert. He graduated from the Department of Physics of Wuhan University in 1925. He was the associate chief designer in three previous projects and the chief designer for another project. He was involved in the development of four large-scale rockets, including the first guided missile that China developed. Jiang Cuoping is a generation behind the two gentlemen mentioned earlier. He graduated from the Beijing Institute of Aeronautics and Astronautics in 1964. Since then, he has been working at the Second Research Institute. He pointed out to the reporters that "the Beijing Simulation Center is here because there is a dedicated technical team. It is centered around old and middle-aged staff members with a large number of young people as its major force. Several hundred people work together to solve key problems."

The first problem encountered by the project was the overall design. Although a large number of countries are engaged in the development of simulation technology, however, it is done in a very secretive way, especially in terms of the overall design and the high technology employed to support the design. There was no reference to rely on. What did we do? There was one way to create it. Nevertheless, it is very difficult to design a feasible design in the mid 80's that will meet the standards in the 90's.

Fang Huihuang summarized this effort in the reception room to reporters as follows. Facing this monumental task, several dozen experts worked very hard for several years based on the principle of aiming at a high starting point and reaching for a giant step forward. Finally, the problem was solved. This is a result of our independent effort after fully understanding the latest information and technology available throughout the world.

Fang stressed the importance of the spirit of independent effort to the project. For instance, the three-axis rotation table was imported before the laboratory was constructed. It was temporarily stored in another room. When it was

time to move it, the foreign manufacturer asked an additional 3 million to 6 million yuan for relocation. This is equivalent to another three-axis rotation table. Xu gathered experts from various fields to evaluate the situation. After a detailed analysis, he made a very risky decision to move the table ourselves. This was a very difficult task for Chinese technicians that did not have the level of sophistication required. A slight mistake could lead to disastrous results. Nevertheless, a technical team led by Senior Engineer Li Yongxin [2621 3057 9515] was able to successfully complete this task in one attempt.

Xu Naiming pointed to the impressive radio-frequency (RF) simulation lab and said that this is a "dual-purpose lab" and for the first time in the world the millimeter wave lab is compatible with microwave lab as well. Back then, the United States had a monopoly on millimeter wave technology. Researchers led by Chen Xunda [7115 6064 6671] thought of a unique method. During the period of a year and a half, the team experienced numerous difficulties and spent long and hard hours day after day in system testing. Because the system is highly complex and large, they often reached a dead end and then discovered a new way out. The dual-purpose lab saved the government approximately 30 million yuan.

Jiang Cuoping mentioned that their hard working spirit moved a number of foreign experts. A young American let a Chinese engineer work while standing on his shoulders. He said that he respects dedicated workers that produce high quality work.

Since the second half of 1992, various government departments and experts conducted a rigorous evaluation of each laboratory and the overall project at the Beijing Simulation Center for over 6 months. On 29 January 1993 and 26 April 1993, it passed the technical part and completed inspection by the State Inspection Commission, respectively. In order to honor the technical staff at the Beijing Simulation Center, the Ministry of Aerospace Industry issued them a collective first place award.

Widespread Applications in the Future

The newly constructed Beijing Simulation Center occupies a total of 13,120 square meters of floor space. It has 11 laboratories. In addition to conducting simulation studies for spacecraft and carries rockets, it is also actively pursuing contracts to perform simulation for major engineering projects in transportation, energy and chemical engineering.

During the construction period, it successfully conducted over 10,000 simulations for the well-known Changzheng (Long March) carrier rocket. Because of numerous simulations performed by the Beijing Simulation Center, the development period for an antiaircraft missile was shortened by 2 years, saving over several tens of millions of yuan of cost. The Beijing Simulation Center also offered its service to the Helongjiang Electric Grid System with regard to questions such as "What are the factors affecting the stability of the power grid?" and "What are the steps to take after an incident occurs?" and the client was satisfied with the outcome. Chief Designer Fang Huihuang confidently indicated that the next step is to contribute to the Three Gorges Project.

Chen Dingchang [7115 1353 2490], director of the Second Research Institute, mentioned in the press conference that the city of Zhuhai is very anxious to employ simulation technology to arrange its transportation routes, gas pipelines and residential areas. The construction of the future bridge between Zhuhai and Hong Kong also needs simulation.

Jiang Cuoping also indicated that the Beijing Simulation Center has received several thousands of foreign experts and government officials to date. A foreign leader praised the Chinese government for making such a smart decision to build such a high standard simulation center staffed with an outstanding Chinese technical team. After visiting the infrared tracking laboratory, a vice president of the Houston Corporation immediately acknowledged that the Chinese version is more rigorous than the U.S. version and expressed a desire to cooperate further.

The staff at the simulation center pointed out that the center is built on a solid foundation and has a good start. They are determined to complete the second phase of construction in order to exceed existing world class level.

PRC-Taiwan Marine Sciences Collaboration

93P60349A Beijing RENMIN RIBAO OVERSEAS EDITION in Chinese 18 Aug 93 p 5

[Article by Cai Guoyan [5591 0948 3533] and Su Dongkun [5685 2639 2492]]

[Summary] In order to enhance China's overall research strength and to promote China's international position in marine sciences by using mainland China's superior research staff, its solid basic research, Taiwan's abundant funds and excellent facilities, the two sides have signed an agreement to conduct scientific research in this area. At the "Marine Sciences of the Taiwan Straits and Vicinity Conference," both sides agreed upon joint study on four projects, which are to achieve definite research results in biological and geochemical studies of the southern East China Sea, to exploit the Nansha Archipelago using PRC-built research ships, to determine the accurate position of each island in the South China Sea using satellite remote sensing facilities developed by the People's Republic of China (PRC), and to conduct hydrological, geological, chemical, and biological studies of the northern South China Sea using ships dispatched by both sides. The next conference will be held in Taipei, Taiwan, in 1994.

More Details on 'Long March 1D'

93FE0970A Beijing HANGTIAN [SPACE FLIGHT] in Chinese No 4, 26 Jul 93 pp 11-13

[Article by Jian Fen [0256 5358] and Hu Xiaodong [5170 2556 2639]]

[Text] The "Long March 1D" (CZ-1D) launch vehicle is an improved model of the "Long March 1" (CZ-1).

The development of China's first space launch vehicle, the "Long March 1," began in 1965. On 24 April 1970, it launched the "Dong Fang Hong 1" satellite, which made China the fifth country in the world to develop its own satellite launch capability. On 3 March 1971, the "CZ-1" launched the "Shi Jian 1" scientific exploration satellite. This launch vehicle can carry a 300-kg payload into a 440-km, 70°-inclination circular orbit.

The "Long March 1" is a three-stage rocket whose first and second stages are three-axis stabilized liquid-propellant rockets, and whose third stage is a spin-stabilized solid-propellant rocket. The CZ-1 is 29.87 m long and has a diameter of 2.25 m; its tail fins are separated by 3.81 m and its lift-off weight is 80,500 kg.

The first two stages of "Long March 1" use self-activated liquid propellant—60,000 kg in the first stage and 10,950 kg in the second stage. The fuel is unsymmetrical-dimethyl hydrazine and the oxidizing agent is nitric acid-27s, both of which are supplied to the engine by pump pressure. The first-stage engine has four nozzles connected in parallel; its total thrust at sea level is 1,020 KN, its specific impulse is 2,349 N s/kg, and its burn time is 140 sec. The second-stage engine has a single fiberglass nozzle designed for high-altitude operation; its thrust in vacuum is 294.2 KN, its specific impulse is 2,746 N s/kg, and its burn time is 102 sec.

The propellant tanks of the first and second stages are made of welded aluminum alloys. The second-stage tank has a "shared conic base" design which directly bears the thrust load of the engine and reduces the overall length and weight of the rocket. The instrument compartment, the inter-tank section and the tail section of each stage are all made of riveted aluminum alloys. The section which connects the first and second stages consists of two halves; the upper half is a cylindrical shell made of aluminum alloy, the lower half is a rod assembly containing 16 alloy-steel rods. During stage separation, the jet flame from the second-stage engine is exhausted through the rod openings.

The third-stage solid-propellant engine of the "Long March 1" is 4.0 m long and has a diameter of 0.77 m; its total weight is 2,056 kg and it is packed with 1800 kg of thiokol composite propellant. The total impulse of the engine in vacuum is 4,440 KN s, and the burn time is approximately 40 sec. Prior to ignition, the four tangential rockets located in the plane which passes through the center of mass are activated, thus initiating the spin of the third stage at 180 rpm. The solid-propellant engine is supported by a conical skirt attached to the second stage. Attached to the forward section of the engine are support frames for the instrument compartment and the satellite. After orbit injection, the satellite is separated from the launch vehicle by an ejector. The entire third stage is enclosed in a fairing 1.5 m in diameter and 4.63 m long. The second stage is separated from the third stage by cold separation technique.

The flight profile of the "Long March 1" can be divided into three segments: power flight segment of the first and second stages, coast flight segment of the second stage and accelerating flight segment of the third stage. With the exception of the third segment which is controlled only by a time command unit, all other segments are controlled by the inertial control system located in the instrument compartment of the second stage. The components of the guidance system include an air-float type gyroscopic longitudinal accelerometer, lateral and normal accelerometers computers and amplifiers. The system uses abridged position compensation technique and coordinate transformation for longitudinal, lateral and normal guidance in order to control the parameters at second-stage engine cut-off so that at the end of the coast-flight segment, the third stage will arrive at the pre-determined position and have the precise velocity prior to ignition. The sensing elements of the attitude control system include a static-pressure air-float type horizontal gyroscope, a vertical gyroscope and a rate gyroscope. During the power-flight segment of the first and second stages, an intermediate device is used to operate two rudders (which in turn drives four gas rudders), and to control the attitude-control solenoid (which controls eight nitrogen nozzles) for pitch, yaw and roll stability.

The "Long March 1" launch vehicle is equipped with a telemetry system and ballistic monitoring and tracking devices. Together with the ground stations along the flight path, they form a comprehensive radio measurement and tracking system. The telemetry system uses a time-division-based composite modulation system (i.e., PACM-FM) to measure more than 330 parameters during flight; the maximum measurement range is 1,800 km. The tracking system uses a continuous-wave (CW) radar for velocity measurement and a monopulse radar for position measurement. The launch vehicle is equipped with a corresponding responder. In addition, a steering radar performs beam-steering to facilitate capturing the target.

The "Long March 1" has an independent self-destruct system. When the attitude of the rocket becomes unstable, the self-destruct contacts on the gyroscope are closed, thereby activating the detonators of the first and second stages, which penetrate the propellant tank and cause an explosion which destroys the rocket in mid air. Once the normal mission of the first and second stages is completed, the self-destruct system is activated through a time-delay system, thereby destroying the rocket to ensure range safety. In addition to the above self-destruct mechanisms, if the rocket trajectory deviates from the designated safety zone, and the error cannot be corrected, then a safety officer on the ground can also issue a self-destruct command to the receiver onboard the rocket via the tracking system.

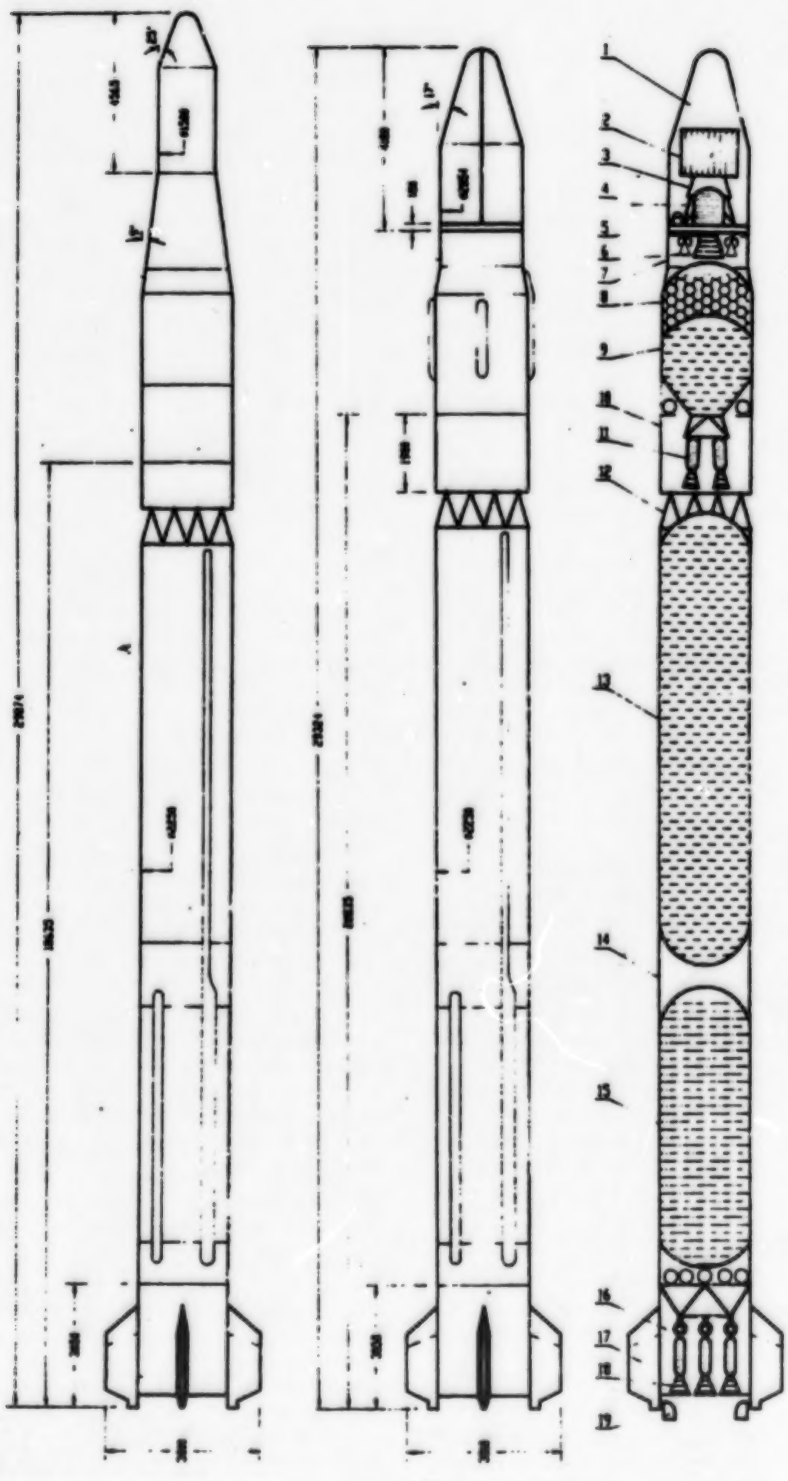

Figure A. Structural Diagrams of the "Long March 1" Family of Rockets

1. Fairing; 2. Typical payload; 3. Payload butt joint (conical transition section); 4. Control and measurement instrument; third stage support frame; 5. Third-stage solid-propellant engine; 6. Engines of the auxiliary propulsion system; 7. Inter-stage section between the second and third stages; 8. Second-stage fuel tank; 9. Second-stage oxidizing agent tank; 10. Inter-stage section between the first and second stages; 11. Second-stage liquid-propellant engine; 12. Rod system; 13. First-stage oxidizing-agent tank; 14. Inter-tank section; 15. First-stage fuel tank; 16. First-stage tail section; 17. Tail fins; 18. First-stage liquid-propellant engine; 19. Gas [internal] rudder

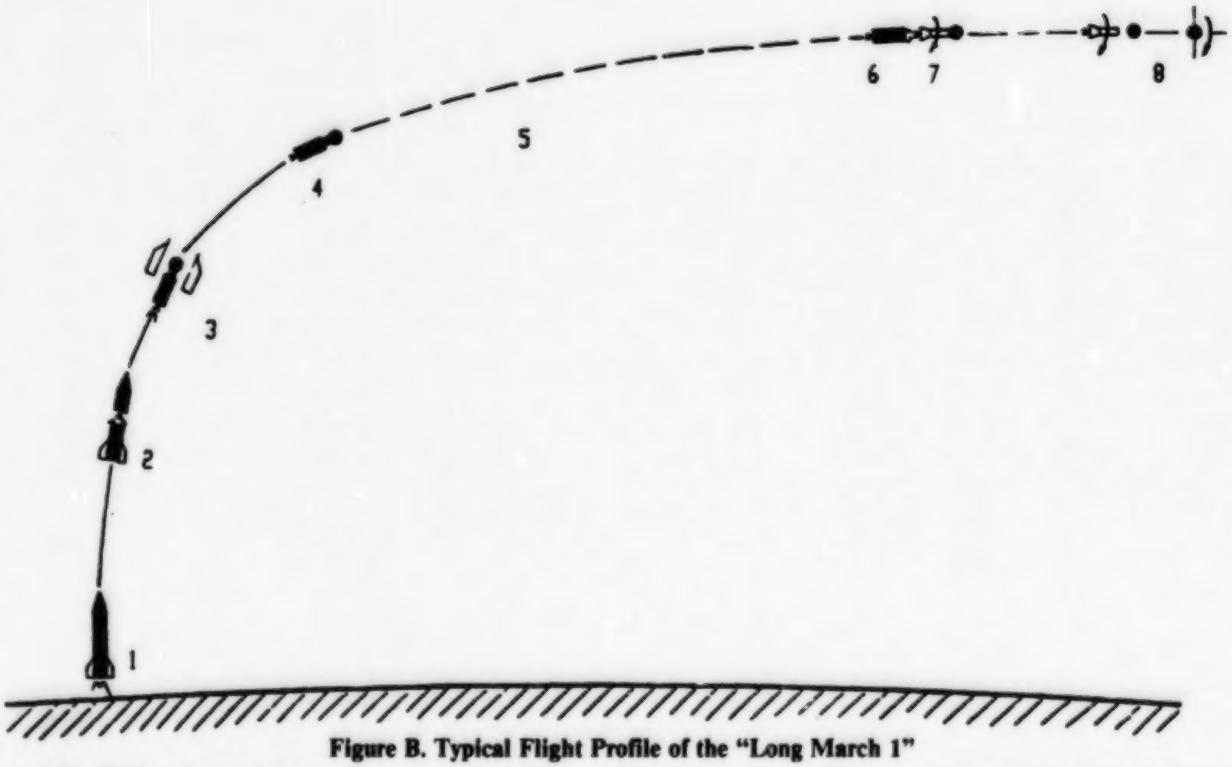

Figure B. Typical Flight Profile of the "Long March 1"

1. Lift-off, T = 0 sec; 2. First-stage engine cut-off, T = 140.43 sec, altitude: 60 km, velocity: 2,132 m/sec; 3. Fairing ejection, T = 161.56 sec, altitude: 80 km; 4. Second-stage engine cut-off, T = 240.36 sec, altitude: 187 km, velocity: 4,788 m/sec; 5. Second-third state coast-flight segment; 6. Third-stage engine ignition, T = 520.19 sec, altitude: 443.9 km, velocity: 4,466 m/sec; 7. Second and third stage separation (T = 513.69 sec), third-stage spin initiation (T = 516.69 sec), third-stage engine ignition (T = 520.19 sec); 8. Satellite separation, orbit injection, T = 579.0 sec, altitude: 452.2 km, velocity: 8,153 m/sec

Development of the "Long March 1D" began in 1987; it was primarily designed to launch small domestic and foreign satellites and various types of sub-orbital experimental payloads. The main improvements made on the "Long March 1D" include the following:

a) The thrust of the first-stage engine has been increased to 81.3 KN; the sea-level thrust is 1,101.3 KN and the sea-level specific impulse is 2,378 N s/kg. The propellant amount has been increased to 64,450 kg.

b) The second-stage engine has been replaced by two parallel swiveling engines, which use dinitrogen tetroxide as the oxidizing agent. The gas rudders have been removed, and the tail section of the second stage is ejected during the stage separation. The propellant amount of the new second stage is 12,100 kg, the total engine thrust is 100.86 KN, the specific impulse in vacuum is 2,971 N s/kg, and the burn time is approximately 360 sec; the maximum composite swivel angle is 5.6°.

c) The third stage is equipped with an advanced solid-propellant engine which uses butyl-hydroxy composite propellant; its specific impulse in vacuum has been increased to 2,834 N s/kg. In addition, a liquid-propellant dual-element auxiliary propulsion system consisting of three sets of 16 multi-starting nozzles has been added to provide the necessary control force and control moment for three-axis stabilization and the required impulse for orbit-transfer maneuvers.

d) An inertial control system with an "abridged rate computer" is used; the system has been relocated to the third stage in order to ensure three-axis stabilization of the payload attitude and to make fine adjustments of the orbit parameters at the time orbit injection.

e) The size of the satellite fairing has been increased; the new fairing, which is 2.05 m in diameter and 4.0 m in height, can accommodate a payload 2.0 m tall and 3.0 m^3 in volume.

The improved "Long March 1D" three-stage rocket is 29.3 m tall and has a lift-off weight of 85,000 kg. It is superior to the "Long March 1" in terms of launch capability and flexibility. Specifically, it can be assembled in three different configurations to accommodate different missions.

a) Single-stage rocket. It is powered only by the first-stage engine, and can launch a 2,200-kg payload vertically to an altitude of 1,000 km to provide 15 minutes of flight time for micro-gravity experiments.

b) Two-stage rocket. It is powered by the first and second stage engines, and can launch a 1,000-kg payload into a 28.5°-inclination, 185-km altitude low-earth orbit.

c) Three-stage rocket. It is primarily used to launch payloads into polar orbits and sun-synchronous orbits. It can also launch payloads into geosynchronous transfer orbits. Since the auxiliary propulsion system has multiple-ignition capability, the three-stage rocket can fly along a Holman transfer orbit; for example, it can launch a 400-kg payload into a 903-km, 99°-inclination sun-synchronous orbit.

Fermenting Genetically Engineered E. coli To Synthesize Cholera Toxin B Subunit

93P60350A Beijing WEISHENGWU XUEBAO [ACTA MICROBIOLOGICA SINICA] in Chinese Vol 33 No 3, Jun 93 pp 177-181

[Article by Yu Xiuqin [0060 4423 3830] and Ma Qingjun [7456 3237 6874]]

[Summary] Having studied the cloning and expression of cholera toxin gene and toxin-deficient A^-B^+ gene, researchers at the Institute of Biotechnology of the Academy of Military Medical Sciences have successfully screened the high-yield E. coli strain MM2 (PMM-CTB) to express cholera toxin B subunit (CT-B). The PMM-CTB was then fermented in a 50-liter MSJ-u3 fermenter containing 3 percent steeped-corn syrup medium to mass-produce the CT-B subunits. The technique can produce up to 40 micrograms of CT-B subunits per milliliter (ug/ml) of medium, the highest output level ever reported. The advantage of using steeped-corn syrup medium is its low cost, convenience, and high yield.

Hepatitis C Diagnostic Reagent Developed

93P60350B Beijing RENMIN RIBAO OVERSEAS EDITION in Chinese 19 Jul 93 p 3

[Article by Wang Yuan Yuan [3769 0954 0954]]

[Summary] An enzyme-linked immunosorbent assay (ELISA) hepatitis C diagnostic reagent has been developed by molecular virologist Ma Xiankai [7456 6343 0418] of the Institute of Basic Medicine, the Academy of Military Medical Sciences (AMMC) of PLA. The reagent has been under clinical trial for more than a year and has been proven to be highly sensitive, highly specific, and stable. To market the product, the institute established a joint venture company with Hong Kong Weique Investment Group Company Ltd., called the Beijing Weikai Medical Biotechnology Company Ltd. The new company will carry out all activities including R&D, manufacturing, production, and marketing of a series of diagnostic reagents, electronic devices for medical use, and other medically related high-tech products for hepatitis and AIDS treatments.

Genetically Engineered Human Erythropoietin

93P60350C Shanghai WEN HUI BAO in Chinese 16 Aug 93 p 1

[Article by Li Tongbin [2621 0681 2430]]

[Summary] A group of researchers headed by Cao Yunxu [2580 7291 2485] of the Institute of Medical Biotechnology and Molecular Genetics of the Second Military Medical University has developed a human Erythropoietin (EPO) using genetic engineering technology. Cell strains constructed by the institute can highly express EPO gene and yield 2,100 to 5,000 units of EPO per milliliter of medium. Results from tests conducted on animal and human bone marrow cells indicate that the newly developed EPO is highly effective. This Chinese-developed drug will be widely used in China to treat anemia resulting from chronic kidney failure.

Natural Nerve Growth Factor Produced

93P60350D Beijing KEJI RIBAO [SCIENCE AND TECHNOLOGY DAILY] in Chinese 27 Jul 93 p 1

[Article by Kou Yong [1379 0516]]

[Summary] Researchers led by Head Engineer Li Yubo [2621 3768 3134] of the Department of Biotechnology Development of the Jiangxi Changsheng Science and Technology Industrial Company, have purified a natural nerve growth factor (NGF) from animal embryos. Results from clinical trial on 50 patients indicate that this pure NGF product is highly effective, non-toxic and costs less than American products. Because NGF can promote regeneration of damaged nerves and revives their functions, it is considered to be essential to the maintenance of normal growth and function of the nervous system. Clinically, NGF has been widely used for treating several neural system diseases such as cerebrovascular diseases (strokes), encephalitis, senile dementia, cerebral dysgenesis, poliomyelitis, sequel of craniocerebral trauma, and malignant tumors.

Chinese-English, Chinese-Japanese MTSs Certified

94p60012B Beijing KEJI RIBAO [SCIENCE AND TECHNOLOGY DAILY] in Chinese 15 Sep 93 p 1

[Article by Zhou Ganpu [0719 2413 2528]: "Chinese-Foreign Machine Translation Breakthroughs Reached"]

[Summary] The commercialized Chinese-English and Chinese-Japanese machine translation systems (MTSs) developed by the China Computer Software and Technical Services Corporation passed the formal technical appraisal conducted by MEI's Computer Department on September 13. As tested by the experts, the Chinese-English MTS has an average translation time of 176 wpm with a readability/understandability of 71 percent, while the Chinese-Japanese MTS has an average translation time of 201 characters/minute with a readability/understandability of 70.5 percent. The Chinese-English MTS has been in trial use at three commercial firms, where it was employed to translate several hundred thousand words of S&T documents.

50-Gigabyte Optical Disk Jukebox Certified

94p60012A Beijing JISUANJI SHIJIE [CHINA COMPUTERWORLD] in Chinese No 32, 18 Aug 93 p 1

[Article by Xu Zhou [1776 3166]: "DE-1000 Optical Disk Jukebox Passes Appraisal"]

[Summary] The model De-1000 optical disk jukebox developed by Qinghua University Microfine Engineering Institute passed the formal technical appraisal jointly conducted by the State Planning Commission and State Education Commission on 12 August. The DE-1000, a system which automatically changes optical disks and reads/writes optical disk information, has a capacity of 47-50 GB (gigabytes) and is compatibale with one-time-writable and erasable rewritable 5.25-inch optical disks, of which it can hold up to 50. Average disk-change time is less than 5 seconds.

Canada's MDA Company Completes Upgrade of CAS Remote Sensing Satellite Ground Station

94P60007B Beijing ZHONGGUO KEXUE BAO [CHINESE SCIENCE NEWS] in Chinese 23 Aug 93 p 1

[Article by Huang Anwen [7806 1344 2429]: "CAS Remote Sensing Satellite Ground Station Upgrade Project Completed"]

[Summary] At a ceremony held in Beijing on 13 August, a project manager of Canada's MDA Co. formally turned over to CAS Remote Sensing Satellite Ground Station (RSSGS) Associate Manager Pan Xizhe [3382 5045 0772] the operation of the newly upgraded facility: a "turn-key" receiving and processing system. This upgrade, supported by the State Planning Commission, State S&T Commission, and national space offices, was a 1-year joint project carried out by engineers on both sides, and permits the CAS RSSGS to receive Landsat-6's 15-meter-resolution ETM imagery as well as synthetic aperture radar imagery from the European Space Agency's ERS-1 and Japan's JERS-1 Earth resources satellites.

Kilowatt-Class CW Oxygen-Iodine Chemical Laser Developed

94P60007C Beijing ZHONGGUO KEXUE BAO [CHINESE SCIENCE NEWS] in Chinese 1 Sep 93 p 1

[Article by Zou Shuying [6760 3219 5391]: "New Chemical Laser: Output Power Reaches 1,000 Watts"; for additional details, see JPRS-CST-92-025, 16 Dec 92 pp 32-37]

[Summary] Dalian, ZHONGGUO KEXUE BAO wire report—The kilowatt-output-power continuous-wave oxygen-iodine chemical laser (COIL) developed by scientists at the CAS Dalian Institute of Chemical Physics passed formal technical appraisal the other day. This new type of high-power chemical laser, with applications in the military, laser inertial confinement fusion, and industrial processing, was developed by the Dalian institute in an 863 Plan project beginning in April 1991. The appraisal experts have certified the COIL's power level, specific power, and chemical efficiency as meeting current international standards for such lasers.

DFB Resonant Cavity Raman Free Electron Laser Oscillator Developed

94P60007A Shanghai ZHONGGUO JIGUANG [CHINESE JOURNAL OF LASERS] in Chinese Vol A20 No 6, Jun 93 p 433

[News brief by Ji Zhong [4764 6988]: "Distributed-Feedback Resonant Cavity Raman Free Electron Laser Oscillator Developed"]

[Summary] The free electron laser (FEL) research group led by CAS Shanghai Institute of Optics and Fine Mechanics (SIOFM) Associate Research Fellow Wang Mingchang [3769 2494 1603] has developed the first distributed-feedback (DFB) resonant cavity Raman FEL oscillator. Main technical parameters of this oscillator are as follows: pulse-line accelerator electron beam energy is 0.4 MeV, beam current is 800 A, laser output pulsed power is 6.6 MW, pulse width is 20 ns, laser wavelength is 8.7 mm, output power at center wavelength is 2.5 times the superradiation [value], and energy conversion efficiency is 2.1 percent. This apparatus's output power is 10 times higher than that achieved in 1990 at Japan's Osaka University. The experts have appraised the SIOFM achievement as meeting 1990s international standards for theoretical analysis and experimental results.

Femtosecond Optical Pulse Dye Amplifier

40100007 Shanghai ZHONGGUO JIGUANG [CHINESE JOURNAL OF LASERS] in Chinese Vol A20, No 5, May 93 pp 326-329

[Text of English abstract of article by Zhang Xiaotian, Zhu Heyuan, et al, Physics Department, Fudan University, Shanghai 200433; MS received 23 Oct 92]

[Text] An experimental four-stage dye amplifier pumped by a Q-switched frequency-doubled Nd:YAG laser with repetition rate of 10 Hz has been constructed. It amplifies 43 fs optical pulses to energy of 100 μJ and pulsewidth of 125 fs. Optical pulses with pulsewidth of 70 fs and peak power of 1 GW have been generated using a four-prism sequence compressor.

Experimental Study of Erbium-Doped Fiber Amplifier Pumped by 1.47 μm Laser Diode

40100002A Shanghai ZHONGGUO JIGUANG [CHINESE JOURNAL OF LASERS] in Chinese Vol A20 No 7, Jul 93 pp 495-497

[English abstract of article by Jiang Xin, Peng Jiangde, et al. of the Department of Electronic Engineering, Qinghua University, Beijing 100084; MS received 14 Jul 92, revised 13 Oct 92]

[Text] Experimental results on all-domestic-made erbium-doped fiber amplifiers (EDFAs) pumped by 1.47 μm laser diode are reported in this paper. Using mode-field matching technique, the fusion loss between standard single-mode fiber (MFD = 9.125 μm) and erbium-doped fiber (MFD = 3.88 μm) decreased to 0.2 dB. Gain characteristics of EDFAs are investigated and small-signal gain of 24 dB has been obtained.

Optical Parallel Fuzzy Logic Implementations Using Shadow-Casting

40100002B Shanghai ZHONGGUO JIGUANG [CHINESE JOURNAL OF LASERS] in Chinese Vol A20 No 7, Jul 93 pp 520-524

[English abstract of article by Zhang Shuqun, Lin Senmao, and Chen Caisheng of the Department of Electronic Engineering, Xiamen University, Xiamen 361005; MS received 14 Jul 92, revised 12 Oct 92]

[Text] A new spatial encoding method is presented to implement optical fuzzy logic gates by using shadow-casting. Seven kinds of fundamental fuzzy logic operations in parallel can be all optically realized with the system proposed in this paper. The experimental results are also given.

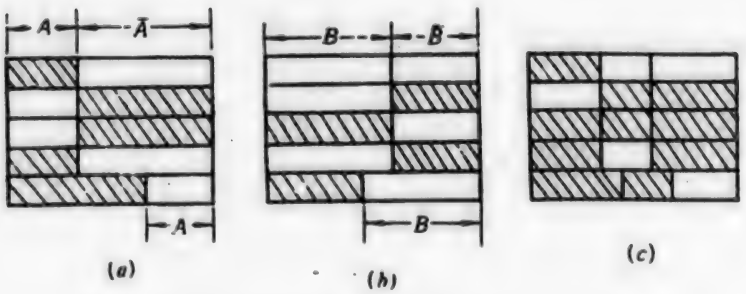

Fig. 1 The spatial encoding method for fuzzy variables

(a) the encoded fuzzy variable A; (b) the encoded fuzzy variable B; (c) the overlap of encoded A and B

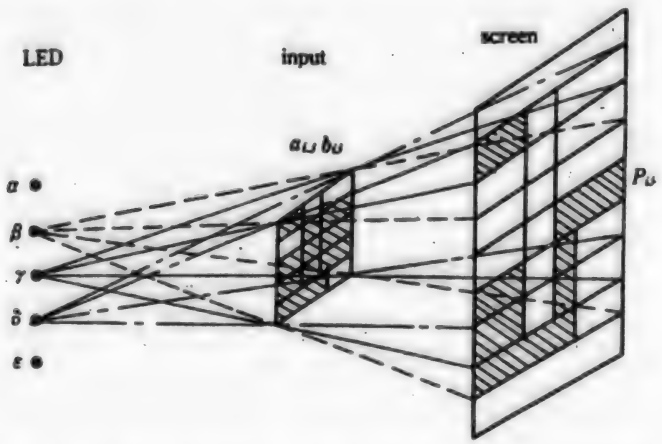

Fig. 2 The optical scheme for fuzzy logic based on shadow-casting

Table 1. The Switching Modes of LEDs and Their Corresponding Operations

Name of implementation	α	β	γ	δ	ε
Complement	+	-	-	-	-
Minimum	-	+	-	-	-
Maximum	-	+	+	+	-
Absoluted-difference	-	-	+	+	-
Implication	+	+	-	-	-
Bounded-difference	-	-	+	-	-
Bounded-sum	-	+	+	+	+

Note: The symbols + and - represent the states of LEDs, on and off respectively.

Reports on Domestic Development of Micromachines

Synchrotron Radiation, LIGA Technique

94P60005A Beijing ZHONGGUO KEXUE BAO [CHINESE SCIENCE NEWS] in Chinese 4 Aug 93 p 2

[Article by Xian Dingchang [0405 7844 2490] of the CAS Institute of High-Energy Physics: "New Opportunity of Synchrotron Radiation in the Field of Industrial Production: A Look at the LIGA Micromachining Fabrication Technique"]

[Excerpts] The two synchrotron radiation facilities completed at Beijing and Hefei provide a new vehicle for the nation's scientific research, and bring a new opportunity in the field of industrial production. [passage omitted]

Here I feel that the application of synchrotron radiation in the LIGA [lithography, electroplating, and plastic forming; acronym from German Lithographie, Galvanoformung, Abformung] technique—a large-scale technology used for fabricating high-aspect-ratio micromachines—can serve as an example and illustrate an enormously important new opportunity. [passage omitted]

The light source most suitable for deep-layer photolithography is synchrotron radiation. The soft-X-ray synchrotron radiation light source now available at the Beijing Synchrotron Radiation Laboratory has a wavelength of about 4 Angstroms, with planned improvements that should bring it down to 2 Angstroms, fully suitable for meeting the needs of deep-layer photolithography. [passage omitted]

Since the completion of the Beijing Synchrotron Radiation State Laboratory, researchers there have been exploring the LIGA technique. Recently, in cooperation with colleagues at the CAS Changchun Institute of Optics and Fine Mechanics (CIOFM), the lab's scientists fabricated 20-40-μm-deep three-dimensional microgears on a photoresist—a very pleasing start. In view of the importance of this technique and the availability at the Beijing facility of a synchrotron source providing a wavelength suitable for LIGA research, as well as with the implementation of some needed measures, one can say that a major opportunity has appeared for industrial technology. We should not lose this opportune moment, but should seize it. As the first step, China is in a position to immediately broaden feasibility studies for this technology; this is quite appropriate and timely.

Piezoelectric-Ceramic-Transducer Micromotor

94P60005B Beijing ZHONGGUO KEXUE BAO [CHINESE SCIENCE NEWS] in Chinese 9 Aug 93 p 1

[Article by Gao Jingtai [7559 2529 3141]: "Ultra-Micromotor Unveiled at Changchun Institute of Optics and Fine Mechanics"]

[Excerpt] An ultra-micromotor using a piezoelectric ceramic as the transducer element was recently developed at the Micromachine Laboratory of the CAS Changchun Institute of Optics and Fine Mechanics (CIOFM). This ultra-micromotor's exterior shape is cylindrical, with a diameter of 3 mm and a length of 5 mm; within the range of 300-3,000 rpm, speed can be regulated bidirectionally in smooth, stepless fashion. Also, power output has been noticeably raised. Under loaded experimental conditions, this motor's maximum output torque measured 8.0×10^{-8} N-m and maximum output power was 1.0×10^{-5} W. After a 100-hour life test, the entire machine showed no noticeable wear or signs of failure. These indicators are in a leading position worldwide for such research, and signify a major step forward toward the functional application of micromachine research.

This research was supported by grants from the National Natural Science Foundation [NSFC] and from the CIOFM Director's Youth Fund. Under the guidance of Micromachine Lab Director and Research Fellow Wang Liding [3769 4539 7844], Lu Qiongying [0712 8825 3853] and his micromotor research group used domestically made materials and techniques, and via repeated testing and exploration overcame numerous theoretical and technical obstacles involving materials, fabrication, and experimental technique. [passage omitted]

Micro Polysilicon Beam Switch Vibrator

93FE0825A Beijing BANDAOTI XUEBAO [CHINESE JOURNAL OF SEMICONDUCTORS] in Chinese Vol 14 No 6, Jun 93 pp 331-336

[Article by Sun Xiqing [1327 2569 1987], Li Zhijian [2621 1807 1017], and Fei Guifu [6316 0964 3940] of the Institute of Microelectronics, Qinghua University: "Micro Polysilicon Beam Switch Vibrator"; MS received 23 Apr 92, revised 7 Sep 92]

[Text] **Abstract**

A novel polysilicon beam electrostatic microswitch structure is presented. An effective static analysis of the force bending and electrostatic switching of the polysilicon beam with a fixed boundary tension has been performed.

A low-cost micro polysilicon beam electrostatically driven vibrator is obtained by utilizing the electromechanical process of charge-and-switch-on and discharge-and-switch-off. Preliminary results show that vibration frequency of the beam is approximately 2.1 kHz and the vibration amplitude is very small. The vibration balance point is close to the lower electrode.

I. Introduction

In recent years, much progress has been made in silicon micromachining. The widespread use of a variety of microstructures leads to the introduction of a number of novel devices, including micromechanical devices such as micromotors, micropumps and microrollers[1] and sensors such as acceleration, pressure and flow transducers.[2-4] In addition, micromechanical structures can also be used in dynamic RAMs,[5] vacuum electron devices[6] and silicon beam vibrators.

A silicon microbeam is a relatively simple micromechanical structure. Its mechanical vibration may be thermally, piezoelectrically, magnetically or electrostatically driven. In particular, the electrostatically driven mode is most attractive. Because of its simple structure, the electrostatically driven polysilicon beam can be conveniently used in a variety of harmonic transducers.[7] One of the unique features of a harmonic transducer is its digital output. This can reduce the quantification requirement at the interface.

However, the disadvantage is that it requires a more complicated feedback circuit and capacitance testing structure.

Methods used to analyze balanced bending of electrostatically driven silicon beams primarily include the finite element method,[9] effective mechanical force method[5] and minimum potential method.[10] The first two methods analyze the bending of the polysilicon beam by separating the elastic field from the electrostatic field and result in larger errors. The minimum potential method derives the balanced bending of the beam using the minimum potential principle by taking into account the interaction between the electrostatic field and elastic field. This is a more accurate method. Nevertheless, the result shown in reference 10 is only valid when the deflection of the polysilicon beam is very minute. It does not apply to situations where the bending is large, even to the point where contact is made with the lower electrode, because the contribution of fixed boundary tension is not considered.

In addition to resonance, electrostatically driven polysilicon microswitches have a charge-to-switch-on feature. When the potential between the two electrodes exceeds a certain value, the polysilicon beam bends downward to come in contact with the lower electrode. Then, it is discharged and the beam bounces back under the action of the elastic recovery force. On the basis of this feature, a novel polysilicon non-resonant vibration mode is proposed. This vibration mode is independent of any capacitance testing structure and amplifier circuit. Therefore, the structure and circuitry of the vibrator can be significantly simplified to lower cost.

The second and third part of the paper address the theory of the electrostatic microswitch and the operating principle of the microbeam vibrator, respectively. The fourth part describes the fabrication technique of the electrostatic microswitch and the experimental results of the polysilicon beam vibrator.

II. Theoretical Analysis of Electrostatic Microswitch

Figure 1 shows the basic structure of an electrostatic microswitch. The upper electrode is an elastic polysilicon beam and the lower electrode is the silicon substrate. Both ends of the beam are supported by a Si_xN_y insulation layer. The basic characteristic of the electrostatic microswitch is that the polysilicon beam bends downward, even coming into contact with the lower electrode to discharge, when there is a potential difference between the two electrodes.

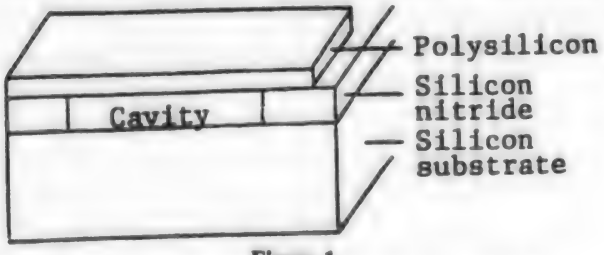

Figure 1.
Basic Structure of an Electrostatic Microswitch

In order to describe the bending of the polysilicon microbeam in the electrostatic-elastic field, it is assumed that (1) the thin polysilicon beam material is uniform, (2) both ends of the beam are rigidly fixed, and (3) the divergence of the electric field between the electrodes is negligible. Hence, the bending of the polysilicon beam under the influence of the field described above can be simplified as a one-dimensional problem, as shown in Figure 2.

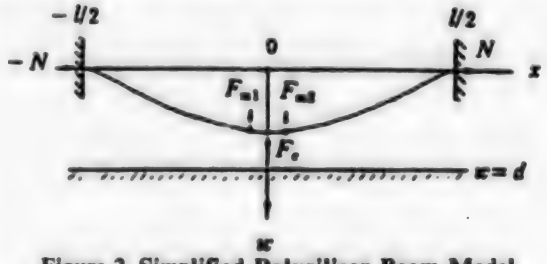

Figure 2. Simplified Polysilicon Beam Model

Let the axial tension of the beam be N, the deflection at any point w(x), center deflection w_1, beam length l, width b, thickness h, and spacing between electrodes d, then the balanced deflection of the polysilicon beam can be expressed in approximation as follows:[1]

$$w(x) \approx w_1 \cos^2 \frac{\pi x}{l}. \qquad (1)$$

The elastic potential of the beam includes two components, i.e., U_{m1}, the distortion energy caused by the axial force N, and U_{m2}, the distortion energy caused by transverse bending. Correspondingly, the elastic recovery force of the polysilicon beam also consists of two components, i.e., F_{m1} due to the axial force and F_{m2} due to transverse bending. They are expressed as follows:

$$U_{m1} = \frac{hE}{1}\left(\int_{-l/2}^{l/2} \left(\frac{dw}{dx}\right)^2 dx\right)^2, \qquad (2)$$

$$U_{m2} = \frac{EJ}{2}\left(\int_{-l/2}^{l/2} \left(\frac{d^2w}{dx^2}\right) dx\right)^2, \qquad (3)$$

$$F_{m1} = -\frac{dU_m}{dw_1} = -\frac{1.5\pi^4 w_1 EJ}{l^3}(w_1/h)^2, \qquad (4)$$

$$F_{m2} = -\frac{dU_m}{dw_1} = -\frac{2\pi^4 w_1 EJ}{l^3}, \qquad (5)$$

where E is Young's modulus and J is the rotational inertia ($= bh^3/12$).

If the voltage between the two electrodes is V, then the electrical energy stored between the two electrodes and the effective Coulombic force are:

$$U_e = \frac{1}{2}\int_{-l/2}^{l/2} \rho V \, dx, \tag{6}$$

$$F_e = -\frac{dU_e}{dw_1} = \frac{C_0 V^2}{4d(1 - \frac{w_1}{d})^{3/2}}, \tag{7}$$

where ρ is density of the line of charge on the electrode and C_0 is the balanced capacitance of the switch ($= \varepsilon_0 lb/d$).

Obviously, the combined force of the polysilicon beam system is:

$$F = F_{m1} + F_{m2} + F_e \tag{8}$$

Figure 3 shows some qualitative curves of F_e and F_m ($F_{m1} + F_{m2}$) at different voltages. One can see that there is always a critical value, V_t, in the polysilicon beam system: the beam meets its mechanical balance condition when $V < V_t$. However, when $V > V_t$, there is no balance point at all and the upper electrode will touch the lower electrode. This critical point can be expressed as follows:

$$\begin{cases} F_e + F_m = 0, \\ \dfrac{\partial F_e}{\partial w_1} + \dfrac{\partial F_m}{\partial w_1} = 0. \end{cases} \tag{9}$$

V_t and its corresponding center deflection w_t can be determined by solving this set of equations.

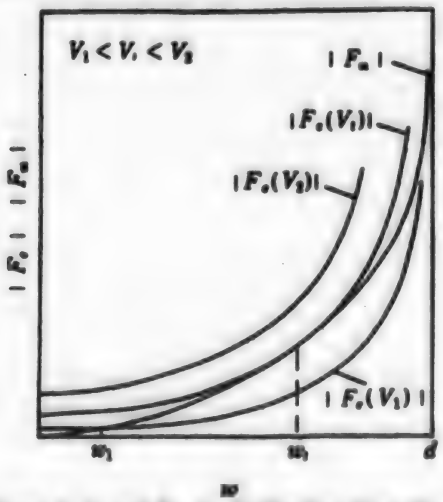

Figure 3. F_e and F_m vs. Deflection Over the Range of [0, d]

With regard to the closure voltages, V_t, for beams of various lengths, some experimental and theoretical work was done and the results are shown in Figure 4. "+" represents measured data, the solid line is derived from equation (10), and the dotted line represents the simulation done in reference 10 where F_{m1}, the axial term of N, is not taken into account. It is apparent that the solid line can better describe the closure voltage of the polysilicon beam as a function of its length. This indicates that the contribution from the axial term F_{m1} can no longer be neglected in the treatment of the closure process of an electrostatic switch.

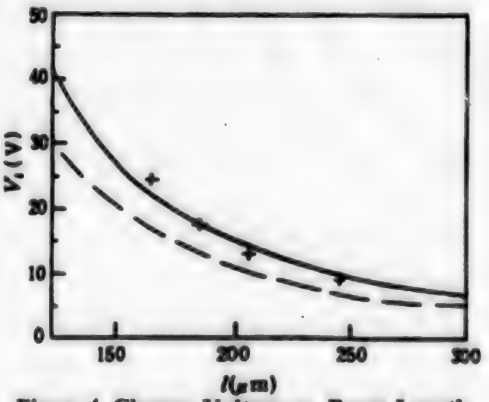

Figure 4. Closure Voltage vs. Beam Length ($b = 25$ μm, $d = 1.1$ μm, $h = 1$ μm)

III. Principle of Operation of the Polysilicon Beam Vibrator

Figure 5 shows the circuit of the polysilicon beam vibrator. The electrostatic switch is a key component of the vibrator. Its capacitance is expressed as C_x, which is approximately under 0.1 pF. In order to adjust the tuning frequency range and to eliminate any nonlinear effect introduced by varying C_x, a larger capacitor C_r ($>> C_x$) is put in parallel with C_x on both sides and the total capacitance $C \approx C_r$.

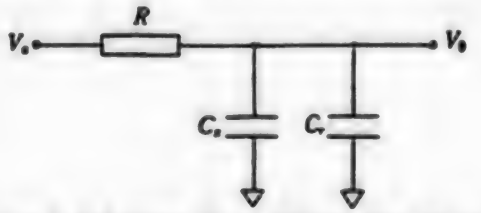

Figure 5. Polysilicon Beam Vibrator Test Circuit

The vibration of the beam is produced as follows. A dc power supply V_s is used to charge the switch through resistor R. When the switching voltage reaches the closure voltage V_t, the upper electrode bends downward to touch the lower electrode to discharge the switch. Then, it springs back up under the action of the elastic recovery force. This electromechanical process is repeated periodically to generate a continuous sawtooth wave.

The charging process of the switch can be expressed as follows:

$$V_0 = V_s + (V_s - V_s)(1 - \exp(-t/RC_r)). \tag{10}$$

When $V_0 = V_t$, the switch closes. Hence, the charging rise time can be expressed as follows:

$$t_r = RC_r\ln(V_a - V_s/V_a - V_t), \qquad (11)$$

where V_s is the starting voltage when charging begins.

If the discharge process of the switch is considered to be very short, then the vibration frequency of the polysilicon beam is:

$$f \approx 1/t_r \qquad (12)$$

When the voltage is relatively large, the formula above becomes:

$$f \approx V_a - V_s/RC_r(V_t - V_s). \qquad (13)$$

The vibration frequency is linear with respect to the voltage.

IV. Experimental Study and Discussion

(1) Fabrication of the Electrostatic Microswitch

Figure 6 shows a cross section of the electrostatic microswitch. Its fabrication technique involves (1) depositing a 3,500-Angstrom-thick layer of Si_xN_y film on a nitrogen-treated N-type silicon substrate, (2) growing a 1.1-μm-thick SiO_2 sacrificial layer and injecting a large amount of phosphorus into SiO_2 to accelerate the etching rate of the sacrificial layer, (3) depositing a 1-μm-thick layer of P-doped polysilicon with a block resistance of 20 Ω/square and rapidly annealing it to relieve the intrinsic mechanical stress of the polysilicon and fabricate the upper electrode by lithography, (4) sputtering aluminum and preparing the welding pad, then applying a gel to protect the electrical contacts before etching out the SiO_2 sacrificial layer to form the electrostatic microswitch structure shown in Figure 7. The dimensions of the microswitch are: l = 50-250 μm, b = 25 μm, h = 1 μm and d = 1.1 μm.

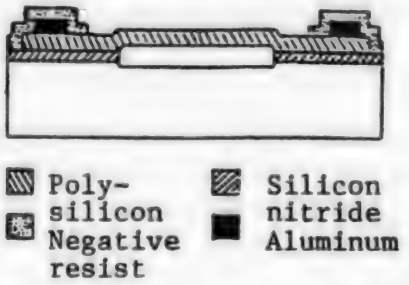

Figure 6. Cross Section of the Polysilicon Beam

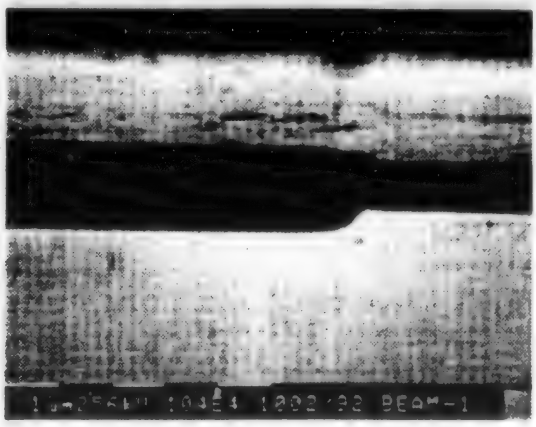

Figure 7. SEM Photo of the Electrostatic Microswitch

(2) Vibration Characteristics of the Polysilicon Beam

The output of the polysilicon beam vibrator shown in Figure 5 was measured in this work using R = 25 kΩ and C_r = 0.1 μF. Figure 8 depicts the output waveforms of the vibrator at different frequencies. Photograph (a) shows the exponential charging process of the switch when the vibrator begins to oscillate. The effect of discharge on the return of the sawtooth wave with a large bias is apparent in photograph (b). At this time, the vibration frequency is 1.7 kHz. In addition, from Figure 8, the peak of the wave is V_t = 17.8 V and the trough of the wave is V_s = 12.9 V. Figure 9 shows the voltage versus frequency curve of the polysilicon beam vibrator. The solid line represents theoretical values calculated based on equation (12). The highest frequency measured is 2.1 kHz. The discrepancy between calculated and measured values becomes larger at higher frequencies. This is because the effect of the discharge process is not taken into account in equation (12).

The charge and discharge of the switch is a highly complex electromechanical process. With the aid of an optical microscope to observe the mechanical vibration of the polysilicon beam, it was discovered that its equilibrium point is close to the lower electrode. Furthermore, the amplitude is very small. Upon closure as a result of charging, the beam merely bends slightly downward to cause the two electrodes to come into "contact" to discharge. In reality, it does not require actual physical contact to discharge because the gas between the two electrodes will be ionized when the field strength exceeds 10^8 V/m. However, not all the charges are removed after a gas-phase discharge. Hence, it still maintains a high voltage V_s (= 12.9 V). In this case, there is no more discharge between the two electrodes, or the rate of discharge is lower than that of charging. Since charging covers the entire polysilicon vibration process, the beam will stop vibrating and remains in the "1" state when the voltage V_a is too high. At this time, $V_a - V_t$ = 36 V. It will heat up if the voltage increases further, eventually leading to plastic deformation of the polysilicon beam.

Stability of micromachined components is an issue of frequent concern. After repeated measurements over long periods of time within the chosen charging voltage range, the behavior of the polysilicon beam vibrator investigated in this study did not show any deterioration.

Since the vibration frequency of the microbeam is a function of resistance R, capacitance C_r, and charging current I, the microbeam vibrator is capable of detecting for a variety of transducers such parameters as resistance, capacitance, and current and providing a digital output.

(a) f=210Hz

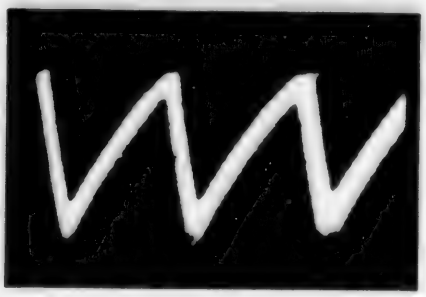

(b) f=1.6kHz

Figure 8. Photographs of Output Waveforms of the Polysilicon Beam

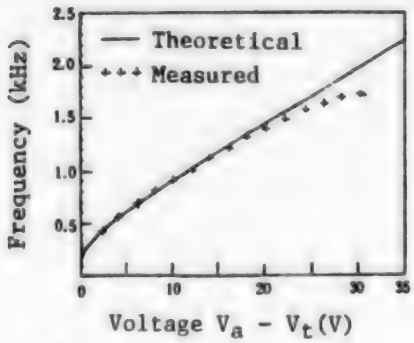

Figure 9. Output Characteristics of the Polysilicon Vibrator

V. Conclusions

(1) A theoretical model that is capable of computing the transverse bending and closure voltage of an electrostatic microswitch is derived by taking axial tension into consideration. It is found that calculated and measured results are qualitatively in good agreement.

(2) A novel polysilicon vibrator has been developed by utilizing the electromechanical process of charge-to-close and discharge-to-open in an electrostatic microswitch. The output frequency of the vibrator is controlled by the operating voltage. Because the design is not optimized, the maximum frequency of the vibrator developed is only 2.1 kHz. More improvement is required.

Acknowledgment

The authors wish to express their gratitude to Associate Professors Zheng Xinyu [6774 1800 3974], Liu Litian [0491 3810 1131], and Xiong Dajing [3574 1129 5464] of the Institute of Microelectronics, Qinghua University, for their assistance.

References

1. R. S. Muller, SENSORS AND ACTUATORS, A21-A23, 1 (1990).

2. B. Puers, L. Reynaert, et al., IEEE TRANSACTIONS ON ELECTRON DEVICES, 35, 764 (1988).

3. J. R. Mallon, Jr., et al., SENSORS AND ACTUATORS, A21-A23, 89 (1990).

4. E. Yoon and K. D. Wise, IEDM 88, p. 670.

5. B. Halg, IEEE TRANS. ELECTRON DEVICES, ED-37, p. 2230 (1990).

6. H. H. Busta, J. E. Pogemiller and M. F. Roth, IEDM 89, p. 533.

7. C. Linder and N. F. De Rooij, SENSORS AND ACTUATORS, A21-A23, 1053 (1990).

8. M. W. Putty and S. Chang, SENSORS AND ACTUATORS, 20, 143 (1989).

9. S. C. Jacobsen, R. H. Price, J. E. Wood, T. H. Rytting and M. Rafaelof, SENSORS AND ACTUATORS, 20, 17 (1989).

10. H. Fujita and T. Ikoma, SENSORS AND ACTUATORS, A21-A23, 215 (1990).

11. Zhang Fufan [1728 4395 5400], "Elastic Plates," Science Publishing House, 1984, p 22.

Flow-Velocity Sensor

93FE0921A Beijing BANDAOTI XUEBAO [CHINESE JOURNAL OF SEMICONDUCTORS] in Chinese Vol 14 No 7, Jul 93 pp 450-452

[Article by Huang Jinbiao [7806 6855 1753], Feng Yaolan [7458 5069 5695], and Tong Qinyi [4547 0530 5030] of the Microelectronics Center, Southeast University, Nanjing and Luo Zhiqiang [7482 1807 1730] of Shenzhen Nanhai Oil Company, supported by the National Natural Science Foundation and the Doctoral Foundation of the State Education Commission: "Flow-Velocity Sensor Fabricated by Surface Micromachining Technology"; MS received 16 Dec 91, revised 19 Mar 92]

[Text] **Abstract**

This paper presents a polysilicon bridge fabricated by micromachining technique and its application as a flow-velocity sensor. The "bridge body" and "bridge pier" are made of polysilicon and silicon dioxide, respectively. The experimental results show that the output is as high as 380 mV at a flow velocity of 10 cm/s.

In the past 20 years, silicon micromachining technology has made gigantic strides.[1] On the basis of technique, it can be divided into bulk micromachining and surface micromachining. The latter has recently received widespread interest[2] because it can be implemented using single-side lithography (the former requires double-side photolithography), the process is simple and it is highly compatible with IC technology.

The polysilicon bridge resistor designed is shown in Figure 1. The process primarily involves: (1) growing a silicon dioxide layer (approximately 1 μm), (2) growing a polysilicon (0.7 μm) layer by LPCVD with doping, photolithography and annealing, (3) photo-resist masking and selective etching of silicon dioxide to form the bridge structure as shown in Figure 1(c). The polysilicon strip is the "bridge body" and the silicon dioxide on either side is the "bridge pier." Figure 1(d) is a top view of this structure. This bridge design has been adopted, instead of direct deposition of polysilicon on the substrate, based on heat-capacity concerns. This is a compact design with minimal heat capacity. Furthermore, the bridge is thermally insulated from the substrate and has a high thermal sensitivity and desirable dynamic characteristics. The polysilicon strip is 16 μm wide and 160 μm long by design. The strip is unevenly doped, i.e., lightly doped in the middle (region L_c in Figure 1(d)) and heavily doped elsewhere. This uneven doping is adopted based on the following considerations: (1) A higher-sensitivity sensor can be obtained because the temperature coefficient of resistance (TCR) is larger for lightly doped polysilicon. (2) Not only the temperature sensitivity of the polysilicon resistance but also its heating characteristics (which will be described later) can be used for flow-velocity sensing. The temperature rise of such a device upon heating is primarily concentrated in the lightly doped, high-resistance region in the middle. Thus, heat loss to the substrate by way of "bridge piers" can be reduced.

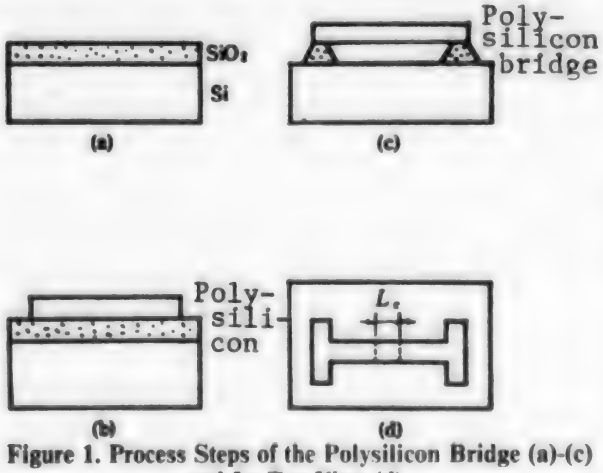

Figure 1. Process Steps of the Polysilicon Bridge (a)-(c) and Its Top View (d)

Polysilicon resistance is comprised of two components: grain resistance and grain boundary resistance.[3] Grain boundary resistance plays a major role in lightly doped polysilicon because it has a larger negative TCR. Figure 2 shows the circuit of the flow-velocity sensor that is based on the temperature sensitivity of lightly doped polysilicon. In the figure, R is the polysilicon thermal resistor, R_1-R_3 are external precision resistors, and A is an operational amplifier. The four resistors form a Wheatstone bridge and the operational amplifier provides amplification and feedback. The sensor operates on the principle of a constant-temperature hot wire anemometer.[4] Specifically, R is heated under the influence of the bridge current. When the flow-velocity varies (e.g., increases) across this resistor, the temperature of R (decreases) and its resistance (rises) are affected. This causes the bridge to deviate from its original equilibrium. The voltage between B and C changes (increases). This change is fed back to A by the operational amplifier to restore the bridge to its original equilibrium. By this time, the temperature (increases) and resistance (decreases) of resistor R change back to their original values. This ensures that R operates at a constant temperature. the output of the operational amplifier reflects any change in flow velocity.

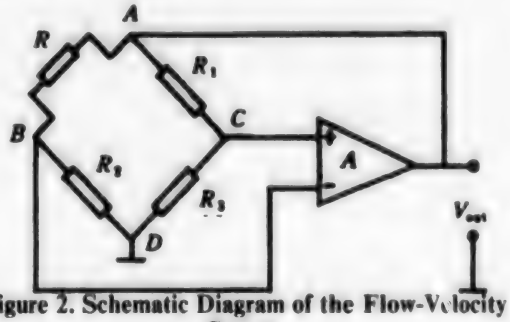

Figure 2. Schematic Diagram of the Flow-Velocity Sensor

The relation between the sensor output V_{out} and flow velocity V_f can be derived from the conservation of energy theorem:

$$V_{out} = c\,(a + b\sqrt{V_f})^{\frac{1}{2}}, \qquad (1)$$

where a and b are heat transfer constants, and c is a constant dependent upon various resistor values, operating temperature of the thermistor and the TCR. The equation indicates that the output of the sensor is a function of flow velocity.

Experimentally, it was found that the TCR of the polysilicon bridge thermistor fabricated is approximately -1200 ppm/°C at near 20°C. A flow-velocity sensor constructed with such a polysilicon thermistor according to Figure 2 was tested in a nitrogen flow environment. Figure 3 shows the experimental results at different flow velocities. From the figure, one can see that the sensor has a high sensitivity. At a flow velocity of 10 cm/s, the output is 380 mV. Since equation (1) can be expressed in terms of a power expansion approximation at low velocities, the results are in excellent agreement with the projected values calculated from equation (1). Dynamic data obtained indicates that the time constant of the sensor is of the order of 1 second,

better than other comparable sensors. Further tests are underway to determine its characteristics.

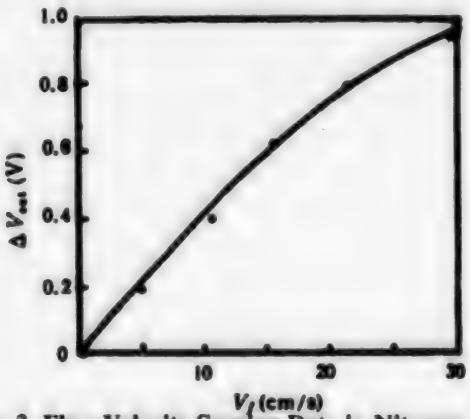

Figure 3. Flow-Velocity Sensing Data in Nitrogen Flow

In addition to temperature sensitivity, polysilicon can also be designed for pressure and light sensing. Because polysilicon fabrication is completely IC-compatible, polysilicon-based sensors can more readily be integrated; i.e., signal processing circuits can be incorporated on the same chip to further improve the performance and flexibility of the sensor.

References

1. R. Rudolf and J. Berggvist, MICROELECTRONIC ENGINEERING, Vol 15, 1991, p 399.

2. Ge Wenxun [5514 2429 8113], YIBIAO JISHU YU CHUANGANQI [INSTRUMENT TECHNOLOGY AND TRANSDUCERS], No 1, 1989, pp 20-22.

3. B. Luder, SENSORS AND ACTUATORS, Vol 10, 1986, p 9.

4. Sheng Senzhi [4141 2773 5347], et al., "Flow Velocity Measurement Techniques," Beijing University Press, 1987, p 45.

5. Huang Jinbiao, et al., BANDAOTI XUEBAO [CHINESE JOURNAL OF SEMICONDUCTORS], Vol 10, No 1, 1989, p 55.

Silicon-Based Electrostatic Micromotor

93FE0521B Beijing BANDAOTI XUEBAO [CHINESE JOURNAL OF SEMICONDUCTORS] in Chinese Vol 14 No 7, Jul 93 pp 453-455

[Article by Sun Xiqing [1327 2569 1987], Li Zhijian [2621 1807 1017], Fei Guifu [6316 0964 3940], and Liu Litian [0491 3810 1131] of the Institute of Microelectronics, Qinghua University: "Silicon-Based Electrostatic Micromotor With Some Structural Improvements"; MS received 23 Nov 92, revised 7 Jan 93. Cf. brief report in JPRS-CST-92-025, 16 Dec 92 p 42]

[Text] **Abstract**

This paper presents an improved silicon-based electrostatic micromotor. On-chip detection of micromotor rotation speed is achieved by fabricating photovoltaic devices on the silicon substrate beneath the rotor. This is very important to the realization of automatic rotation-speed control and fabrication of various sensors. A curved-neck bearing structure that greatly reduces friction torque is fabricated by using a composite sacrificial layer etching technique. The rotors fabricated are 100 and 120 μm in diameter and the layer thickness is approximately 2 μm. Initial tests show that these electrostatic micromotors perform well and have a promising future.

1. Introduction

The advent of microturbines and electrostatic micromotors signifies that research on mechanical microdevices has entered a key stage.[1-3] In particular, mechanical microdevices that are fabricated by IC techniques and can be integrated with sensors and computers on-chip to form complete microelectromechanical systems (MEMS) have attracted the attention of researchers in electronics, mechanical engineering and automatic control.

The key to the realization of closed-loop control is the detection of rotor speed of micromotors and microturbines. Presently, it is accomplished by external imaging methods.[4-6] In this work, on-chip rotor speed sensing is achieved by means of integrated photovoltaic devices.

An important approach to improve rotor behavior is to minimize the contact between the rotor and the bearing and that between the rotor and the substrate.[3,5] In this work, a curved-neck-shaped bearing is fabricated by using a SiO_2/PSG [phosphosilicate glass] composite film sacrificial-layer etching technique. This ensures that there is no contact between the rotor and the substrate. In addition, the rotor only makes round contact with the bearing itself.

2. Key Fabrication Steps

Figure 1 shows a cross section of the electrostatic micromotor prior to the release of the rotor. Its primary fabrication steps are as follows: (1) Deposit a 1.2-μm-thick Si_xN_y/SiO_2 composite layer on the P-Si substrate for electrical insulation and resistance against hydrofluoric acid etching. (2) Etch the composite layer to form the contact hole in zone N. Deposit P-doped polysilicon as the electrical shield for the rotor and the PN junction of the upper electrode. The PN junction is used to detect the speed of the rotor. (3) Deposit the PSG/SiO_2 composite sacrificial layer and then etch it to form the contact between the stator and Si_xN_y. (4) Lay down P-doped polysilicon and etch out the stator and the rotor. (5) Dissolve the sacrificial layer in BHF. The curved neck is obtained as a result of lateral etching because the etching rate of PSG in BHF is very different from that of SiO_2. (6) Deposit SiO_2 and etch the bearing contact hole. Then, deposit a P-doped polysilicon curved bearing. Finally, drop the silicon chip in hydrofluoric acid to release the rotor. Figures 2 (a) and (b) are SEM photographs of the electrostatic micromotor. Photo (a) shows that the rotor is lifted from the substrate by the bearing. The rotor plates and photovoltaic device plates are arranged in an alternating manner. Photo (b) shows that the curved-neck bearing and the rotor's bottom surface only make circular line contact, instead of spherical surface contact. With a weak flow of gas, the rotor begins to spin.

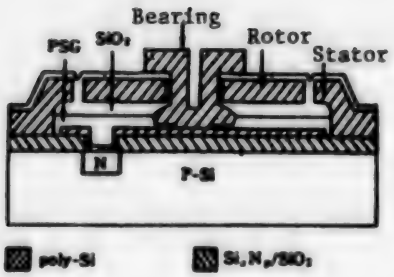

Figure 1. Cross Section of the Electrostatic Micromotor

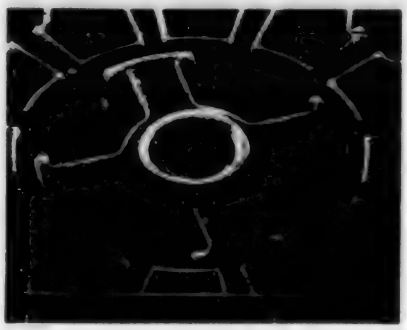

(a) Overall structure

(b) Bearing structure

Figure 2. SEM Photographs of the Electrostatic Micromotor

3. Measurement Principle and Results

Figure 3 shows the motor rotation-speed test setup. A beam of parallel light is shone perpendicularly upon the rotor plane. A three-phase pulse is employed to drive the rotor. When the rotor rotates, the photovoltaic device is either receiving or not receiving light and its output is at either the "high" or "low" level. As the rotor turns one revolution, it produces an electrical signal equal to the number of poles of the rotor. The rotation speed of the micromotor can be determined by counting these electrical pulses.

The three-phase driving voltage arrangement is shown in Figure 3. The 12 stators are divided into four groups. Each pole of the rotor corresponds to a three-phase signal.

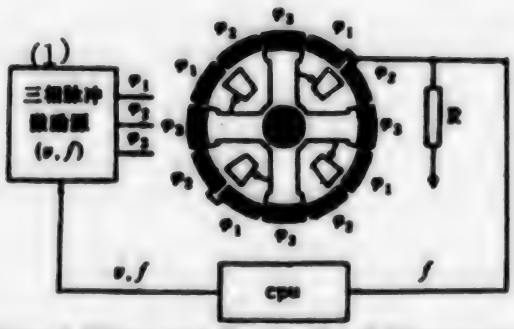

Figure 3. Micromotor Rotation-Speed Measurement System

Key: 1. Three-phase excitation source

During testing, the phase voltage is initially set at a certain value. The phase frequency is then continuously changed until motor rotation is detected. Preliminary results on an electrostatic micromotor with four rotors, 12 stators and a minimum stator-to-rotor gap of 2 μm show that at a minimum driving voltage of 93 V, the maximum rotation speed is 253 rps. At a sustained speed of 100 rps, the micromotor can operate continuously for 14 minutes.

When the motor rotates steadily at 100 rps, once the excitation voltage applied to the stator is removed, it will automatically slow down and stop due to damping. Micromotors of various bearing designs have been tested and the results show that the damping time of the micromotor with the curved-neck bearing described above is 18 ms. This indicates that its damping action is far less than that of a conventional micromotor with a contact bearing design.

The authors wish to express their gratitude to Associate Professors Zhang Jisheng [1728 4949 4141] and Xiong Dajing [3574 1129 5464] for their assistance and to Lin Hong [2651 1347] and Zhong Yan [6988 3601] for their cooperation in device fabrication.

References

1. L.-S. Fan, Y.-C. Tai and R. S. Muller, SENSORS AND ACTUATORS, 20, 41 (1989).

2. M. Sakata, Y. Hatazawa, A. Omodaka, T. Kudoh and H. Fujita, SENSORS AND ACTUATORS, A21-A23, 168 (1990).

3. M. Mehregang, S. D. Senturia, H. Lang and P. Negarkar, IEEE TRANS. ELECTRON DEVICES, ED-39, (9), 2060 (1992).

4. K. J. Gabriel, F. Behi, R. Mahadevan and M. Mehregang, SENSORS AND ACTUATORS, A21-A23, 184 (1990).

5. Y.-C. Tai and R. S. Muller, SENSORS AND ACTUATORS, 20, 49 (1989).

6. S. F. Bast, M. Mehregang, L. S. Tarrow, Jeffrey H. Lang and S. D. Senturia, IEEE, ED-39 (3), 566 (1992).

Study of 1.35 μm InGaAsP/InP Quantum Well Structure Grown by LPE

40100001A Beijing BANDAOTI XUEBAO [CHINESE JOURNAL OF SEMICONDUCTORS] in Chinese Vol 14 No 9, Sep 93 pp 540-544

[English abstract of article by Xing Qijiang, Wang Shumin, et al. of the Department of Physics, Beijing University, Beijing 100087; MS received 27 Jan 92, revised 27 Aug 92]

[Text] 1.35 μm InGaAsP/InP separate confinement single quantum well (SQW) structures have been successfully grown by liquid-phase epitaxy (LPE) technique for the first time in our country. The SQW structures have been studied by the transmission electron microscope cross-section technique and photoluminescence (PL) at 10K and 77K. The well width and transition layer thickness are 160 Angstroms and 30 Angstroms, respectively. The strong free excitonic peaks assigned to the transition between the n = 1 electron quantum level and the n = 1 heavy-(light-) hole quantum level have been observed in the PL spectrum. The photon energy difference between the two photoluminescence peaks is about 8.3 meV, and the full width at half maximum of the PL peak at 10K is 20 meV.

Investigation of Proton Bombardment Mask for InGaAsP/InP PBH CCTS Bistable Lasers

40100001B Beijing BANDAOTI XUEBAO [CHINESE JOURNAL OF SEMICONDUCTORS] in Chinese Vol 14 No 9, Sep 93 pp 562-567

[English abstract of article by Zhang Quansheng, Lu Hui, et al. of National Integrated Optoelectronics Laboratories and Institute of Semiconductors, CAS, Beijing 100083; MS received 23 Jan 92, revised 9 Mar 92]

[Text] A new kind of screen material for proton bombardment, Au/Zn/Au/AZ1350J compound mask which exhibits good screening properties when the bombarding energy is not larger than 250 keV, has been developed based on the study of InP proton bombardment. The technology of making a compound mask for stripe widtj of 5 μm has been resolved for the first time, and InGaAsP/InP PBH common-cavity two-section (CCTS) bistable lasers have been successfully fabricated.

Generation of 1.5 μm High-Repetition-Rate Ultrashort Optical Pulses

40100001C Beijing BANDAOTI XUEBAO [CHINESE JOURNAL OF SEMICONDUCTORS] in Chinese Vol 14 No 9, Sep 93 pp 568-572

[English abstract of article by Xu Baoxi, Gao Yizhi, Li Yanhe, and Zhou Bingkun of the Department of Electronic Engineering, Qinghua University, Beijing 100084; MS received 19 Jun 92, revised 1 Sep 92]

[Text] High-repetition-rate ultrashort optical pulses are generated by gain-switch method at 1.5 μm [InGaAsP laser diode]. The repetition range is from 2.2 GHz to 3.5 GHz, the pulse widths are less than 50 ps.

Preparation of High-Quality Boron-Doped P-Type Semiconducting Diamond Films, Investigation of Doping Behavior

40100001D Beijing BANDAOTI XUEBAO [CHINESE JOURNAL OF SEMICONDUCTORS] in Chinese Vol 14 No 9, Sep 93 pp 579-584

[English abstract of article by Yu San, Zou Guangtian, and Jin Zengsun of State Key Laboratory of Superhard Materials Institute of Atomic and Molecular Physics, Jilin University, Changchun 130023, P. R. China; MS received 31 Jan 92, revised 10 Apr 92]

[Text] Boron doped p-type semiconducting diamond films have been prepared by using the chemical vapor deposition (CVD) method. The crystal structure and lattice spacing of the specimens are the same as that of natural cubic diamond. No excess carbon content was caused by boron doping. The maximum boron concentration in diamond films was measured to be about 10^{20} cm^{-3}. The maximum carrier concentration of holes at room temperature is near 10^{18} cm^{-3}. A sharp peak located at about 1280 cm^{-1} and a broad peak in between 2100-2900 cm^{-1} are observed in IR absorption spectra. This indicates that boron atoms substitute carbon atoms in normal diamond lattice positions and cause an acceptor level of 0.35 eV above the diamond valence band. In addition, a hydrogen-like model of boron atom in diamond also gives that the ionization energy of the acceptors is about 0.35 eV.

Room-Temperature Photoluminescence From Porous Silicon

40100001E Beijing BANDAOTI XUEBAO [CHINESE JOURNAL OF SEMICONDUCTORS] in Chinese Vol 14 No 9, Sep 93 pp 585-587

[English abstract of article by Liu Cheng'en, Zheng Xiangqin, Yan Feng, and Bao Ximao of the Physics Department, Nanjing University, Nanjing 210008; MS received 21 Feb 92, revised 21 Mar 92]

[Text] Electrochemical and chemical disolution was used to prepare high-porosity porous silicon samples at room temperature under excitation of blue light or Ar-laser-beam-emitted visible light. Luminescence spectra were recorded after different period of exposure to ambient atmosphere to show blue-shift and eventual steady state of the spectrum. The total blue-shift of spectrum maximum is about 40 nm. Transmission electron micrograph and electron diffraction pattern of light-emitting film are presented. Both electron micrograph and blue shift can readily be explained by quantum-size effect. Raman spectroscopy measurements show apart from above photoluminescence, a characteristic peak of porous silicon.

Integrated Triple-Drain CMOS Magnetic-Field-Sensitive Transducer

40100001F Beijing BANDAOTI XUEBAO [CHINESE JOURNAL OF SEMICONDUCTORS] in Chinese Vol 14 No 9, Sep 93 pp 588-590

[English abstract of article by Zhang Weixin, Lou Limin, and Mao Ganru of Tianjin University, Tianjin 300072; MS received 27 Jan 92, revised 18 Mar 92]

[Text] A description of the principle of circuit and layout design for a novel integrated triple-drain CMOS magnetic-field-sensitive transducer is presented, and experimental results for the device are also given. The device is noted for its simple circuit structure, high magnetic-field sensitivity and convenience in use. Due to adopting standard CMOS process, it has low price and is suitable for mass-production. It is estimated that the transducers will have a good rate of performance and considerably low price.

All-Digital HDTV for China: Its Parameter Selection, Computer Simulation

40100003A Chengdu DIANZI KEJI DAXUE XUEBAO [JOURNAL OF UNIVERSITY OF ELECTRONIC SCIENCE AND TECHNOLOGY OF CHINA] in English Vol 22 No 4, Aug 93 pp 337-342

[Article by Zhu Weile, Yu Hongyang, and Gu Deren of the Dept. of Electronic Engineering, UEST of China, Chengdu 610054: "An All-Digital HDTV for China: Its Parameter Selection and Computer Simulation"; MS received 30 Nov 92, revised 30 Mar 93]

[Text] **Abstract**

The principles that should be followed in the selection of parameters of HDTV are discussed. A set of parameters based on progressive scanning is proposed. With reference to DigiCipher,[1] all digital source/channel coding and decoding algorithms including motion-compensated inter-frame prediction, fast 2D-DCT [two-dimensional discrete cosine transform], run-length coding and error-protection with RS [Reed-Solomon] (215, 255) codes are implemented. Computer simulation results show that at a compression ratio of 40-60, no noticeable picture degradation is observed. This proves that our simulated HDTV system can work satisfactorily for co-channel broadcasting with the current PAL system.

Key words: TV; high definition TV; image coding; computer simulation; discrete cosine transform (DCT)

HDTV with wide-screen (16:9 aspect ratio) pictures free of artifacts is a new-generation "public medium" accompanying mankind into the 21st century. Through a few rounds of competitions of MUSE, HD-MAC, etc., the all-digital HDTV system, represented by the American [firm General Instruments Corporation's] DigiCipher,[1] is in the leading place of the development of HDTV currently. Incorporating advanced source-coding and channel coding techniques, it is flexible for video-data processing, transmission, storage, and duplication with no noticeable loss of quality. It is also a channel-compatible broadcast system that is especially suitable for China. In order to gain a good grasp of the key techniques of HDTV, a full-length computer simulation of the video codec [coder/decoder] of the HDTV based on DigiCipher was successfully done at UESTC.

However, the current TV system in China is different from that of NTSC, so the parameters proposed by DigiCipher cannot be followed directly. Following the introduction of DigiCipher, some new all-digital HDTV systems have been proposed. Among the four proposed digital HDTV terrestrial broadcasting systems submitted to FCC, two of them use progressive scan with reduced number of scanning lines per frame.[2] In section 1 of this paper, we will review the principles that should be followed in choosing the parameters, and a proposal of parameters pertinent to China will be made. In section 2, the computer simulation of a HDTV system similar to DigiCipher and simulation results are given. In section 3, some key points in the simulation are discussed. Some concluding remarks are given in section 4.

1. HDTV Parameter Selection

For the selection of HDTV parameters, the following factors should be considered.

(1) The resolution should be comparable to that of 35 mm movies—active lines about 1,000 per frame.

(2) Ease of conversion from the current TV system, so that simulcast might be possible with the same studio program.

(3) Channel compatibility, i.e. use of the present 8 MHz channels for PAL-D, or those unused 8 MHz forbidden channels.

(4) Preferably use of progressive scan.

(5) Preferably use of square pixels which is beneficial for easy interface with computers, and use of TV receiver as multi-media terminal.

After careful consideration of all factors, the following HDTV parameters are proposed:

Horizontal scanning rate:
23,437.5 Hz, which is 3/2 of the scanning rate of the current PAL system.

Frame rate:
25 frames/s, progressive scan

Lines per frame:
937/938

Aspect ratio:
16:9

Active video pixels:
1,536 x 864 (luminance) 768 x 432 (chrominance)

Pixel aspect ratio:
1:1

Sampling frequency:
44.25 MHz

Uncompressed data rate:
531 Mb/s

This video data rate is compressed to a data rate of 15 to 18 Mb/s (compression rate of 36 to 30). Together with audio and auxiliary data, the compressed data are to be transmitted within 8 MHz and with 16 QAM [quadrature amplitude modulation]. At the receiver, the video data is to be stored in a frame memory and each frame is displayed two or three times at the field rate of 50 or 75 Hz, so as to reduce flicker. In some more expensive receivers, interpolation can be used to obtain the missing fields. A separate paper has been submitted to ISBT'93, discussing the selection of HDTV parameters in more detail.

2. The Computer Simulation

During the simulation, we used the HDTV sequence of "Un Bel di Vedremo" which originated from RAI. The sequence is composed of frames of 1,440 x 1,152 pixels, interlace scanned. For intraframe imaging coding and motion compensation analysis, four unsampled/trimmed 1,024 x 1,024 pictures and few other still pictures (1,024 x 1,024) are used. In image sequence coding, because of limitations on memory size, we use only the odd fields, down-sampled horizontally. What results is a progressively scanned sequence of 512 x 512 pixels. The reduction of scanning lines will not affect our conclusions drawn from computer simulation, because what is important is the compression ratio attainable which will not degrade the picture quality noticeably.

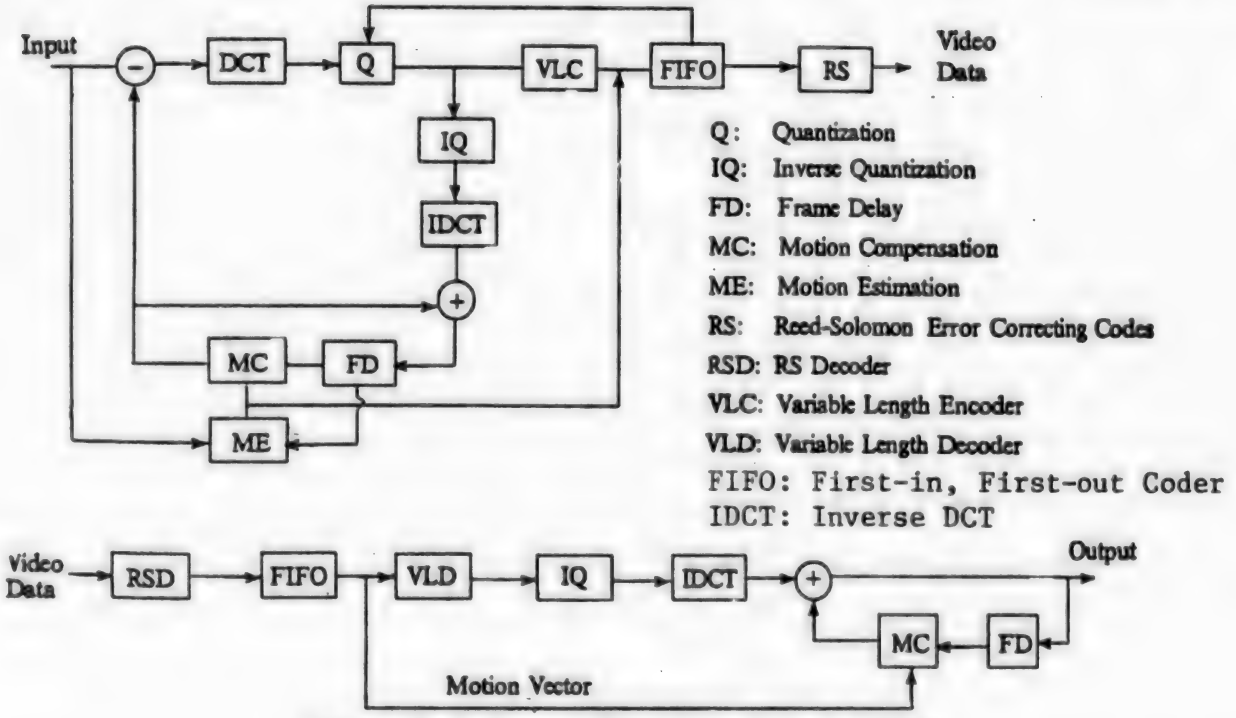

Figure 1. Block Diagram of Digital Video Codec for HDTV

The block diagram for the video codec in the simulation is shown in Figure 1. Audio and auxiliary data transmission are not included in our simulation.

The simulation is carried on a Trapix + 5,500 real-time color image processing workstation with display resolution of 1,024 x 1,024. All the algorithms including fast 8 x 8 DCT, motion detection/compensation, quantization, variable length coding and forward error-correction are implemented. Data after every step are analyzed statistically by special statistical programs. Much experience has been gained through the process. The results show that, for a moving color image sequence, a compression ratio about 1:40 is obtainable while the subjective quality of the images remains excellent. The programs are written in Turbo-C language. We omit the lengthy flow chart here.

3. Some Key Points About Implementation

Not all the algorithms mentioned in Ref. 1 are detailed enough for implementation, and we fill in the gaps whenever this occurs. We also carry out the necessary optimization of the algorithms. The improvement of the algorithms is as follows:

3.1 Motion Detection/Compensation

We use a variable-stage motion search algorithm[3] with minimum absolute difference block matching, which substantially increases the searching and computation efficiency. The block size is 32 x 16, searching range is 54 x 38. The MSE [mean square error] of the frame-differences is shown in Table 1. Because the sequence of "Un Bel di Vedremo" is a picture with a large area of moving people, the result is illustrative.

Table 1. The Comparison of the MSE of Compensated Frame-Difference

	Frame 1-2	Frame 2-3	Frame 3-4	Frame 1-3	Frame 2-4	Frame 1-4
Comp.	48.5	49.0	49.6	55.8	56.4	73.8
Uncomp.	70.1	104.0	73.4	135.5	134.6	210.9

From Table 1, it is seen that the MSE of frame-difference is reduced to 1/3-1/2 by motion-compensation; this renders the possibility of more compression for the following DCT. It is noticed that "false edges" would be introduced by incomplete motion-compensation with mismatch of 2 pixels or more, making the motion-compensation meaningless. The motion-vectors are evaluated on the basis of a superblock with 10-bit representation for each superblock.

3.2 Fast 2D-DCT

Based on the method of fast 1D-DCT in Ref. 4 and fast 2D-DCT in Ref. 5, a fast 2D-DCT algorithm is implemented. The recovery of image data is perfect when floating-point numbers are used; occasionally some 1-level error is introduced when 16-bit integers are used.

3.3 The DC Coefficients

In DigiCipher, the DC coefficient is coded separately by 9-bit code for an 8 x 8 block, which is not a negligible overhead. By statistics, we designed the run-length codebook that reduces the code-length of DCs to 5-6 bits/block.

3.4 Run-Length Coding

Only a combined RI/Amp. code-length table is given in Ref. 1, so we redesign it according to statistics (see Table 2). In our code table, for the lower-order codes the code length remains the same, but for the higher-order codes the code length is much reduced. The new code-length table is shown in Table 2.

Table 2. Number of Bits Used for Each Code Word of Two-Dimensional Huffman Code Book

	Amplitude															
Run length	1	2	3	4	5	6	7	8	9	10	11	12	13	14	15	16
0	2	3	5	5	6	7	8	8	9	9	9	9	9	9	9	9
1	4	5	7	8	9	9	9	9	9	9	9	9	9	9	9	9
2	4	7	8	9	9	9	9	9	9	9	9	9	9	9	9	9
3	5	8	9	9	9	9	9	9	9	9	9	9	9	9	9	9
4	6	9	9	9	9	9	9	9	9	9	9	14	14	14	14	14
5	7	9	9	9	9	9	9	9	9	9	14	14	14	14	14	14
6	7	9	9	9	9	9	9	9	9	14	14	14	14	14	14	14
7	8	9	9	9	9	9	9	9	14	14	14	14	14	14	14	14
8	9	9	9	9	9	9	9	14	14	14	14	14	14	14	14	14
9	9	9	9	9	9	9	14	14	14	14	14	14	14	14	14	14
10	9	9	9	9	9	9	14	14	14	14	14	14	14	14	14	14
11	9	9	9	9	14	14	14	14	14	14	14	14	14	14	14	14
12	9	9	9	9	14	14	14	14	14	14	14	14	14	14	14	14
13	9	9	9	9	14	14	14	14	14	14	14	14	14	14	14	14
14	9	9	9	9	14	14	14	14	14	14	14	14	14	14	14	14
15	9	9	9	9	14	14	14	14	14	14	14	14	14	14	14	14

3.5 Quantization Table

Ten quantization tables are provided in Ref. 1, one of which is selected according to the rate buffer state. The last m bits of the AC coefficient should be masked off according to the value of m shown in the table. An unnecessary inaccuracy is introduced by this method. For example, for m = 6, an AC coefficient of 001111111 is masked to 001 and recovered as 001000000. But, obviously 010000000 is more accurate. So the ordinary "round-off to the nearest integer" method is taken by us, which brings 1-2 dB gain in SNR [signal-to-noise ratio].

3.6 Forward Error-Correction (FEC)

A RS (215, 255) code scheme is applied to the compressed data in code files as channel-coding. It can correct 10 bytes error in a 255-byte (or 512 16 QAM symbols)-long data line. Theoretically, this could enhance a channel with IBER [intrinsic bit error rate] = 10^{-3} to a new BER less than 10^{-5}. But, the effectiveness of the coding scheme can only be verified through field broadcasting.

3.7 Further Improvements

It seems apparent that the lack of adaptivity, both for intraframe and interframe processing, is a deficiency in DigiCipher. For example, a simple quantization scheme is used not only throughout the whole frame, but also for the predictive frames whose statistics are quite different from those of still pictures, indicating an area for improvement. For the motion-vectors, an interframe prediction may be more adequate in speeding up the search process.

4. Conclusions

By computer simulation, the feasibility of an all-digital HDTV codec is fully proved: for still Y picture, a compression ratio about 16-20 is obtained with excellent subjective quality and a PSNR above 31-35 dB; for color still picture, due to the decimation of U, V pictures, the compression ratio is increased to 25-30; and finally, when motion-compensated prediction is used, a total compression ratio about 40-60 is obtained, which is far more than enough to transmit the HDTV signal in an 8-MHz channel. Therefore, the all-digital HDTV system is really an advanced system with high performance. Of course, this simulation is only preliminary. Much more work must be done in the future: Variety of adaptivity to improve the subjective quality of moving-picture sequences, the transmission protocols and system coding, the error resilience whenever a nonrecoverable error occurs, the rate equalization, the FEC field-test, the assessment of picture quality, etc. All these should be studied carefully and then a high-quality HDTV system suitable for China could emerge.

The authors wish to express their sincere thanks to Prof. Xu Mengxia of Beijing University for his valuable comments and suggestions to our original manuscript.

References

1. Woo Paik, "DigiCipher-All—Digital, Channel-Compatible HDTV Broadcast System," IEEE TRANS. ON BROADCASTING, 1990, 36: 245-254.

2. William Y. Zhou, "Comparison of Proposed Digital HDTV Terrestrial Broadcasting Systems," IEEE TRANS. ON BROADCASTING, 1991, 37: 145-147.

3. Kkwatra, S. C., Lin Chowming, Whyte, W. A., "An Adaptive Algorithm for Motion-Compensation Color Image Coding," IEEE TRANS. ON COMMUN., 1987, 35: 747-754.

4. Chen, W. H., Smith, C. H., Fralick, S. C., "Fast Computational Algorithm for Discrete Cosine Transform," IEEE TRANS. ON COMMUN., 1977, 25: 1004-1009.

5. Kamanger, F. A., Rao, K. R., "Fast Algorithm for the 2-D Discrete Cosine Transform," IEEE TRANS. ON COMPUT., 1982, 31: 898-906.

Long-Range Plans for Space Development

93FE0920A Taipei HENENG TIENTI [NUCLEAR CLIMATE MONTHLY] in Chinese
No 6, Jun 93 pp 45-49

[Article by Chang Yuwen [1728 5940 2429]]

[Text] Over the past 2 years, a number of articles on "artificial satellite development" have appeared in local newspapers and magazines; they reflect the strong interest of the Government of the Republic of China (ROC) in space development. By building on its industrial foundation in parts assembly and subsystem development and establishing a comprehensive plan of space development, the ROC will be able to build larger and more complex high-tech systems and to develop the capabilities in design, development and integration.

A space development plan is a multi-element plan that covers many scientific and engineering disciplines; it plays a leadership role in stimulating the development of new technologies and forming new industries. Space development has a unique position in the evolution process of a nation's scientific and technological capability. For this reason, the ROC Government established a national 15-year long-range plan for space technology development in 1991.

Fifteen-Year Space Development Plan

According to this plan, three satellites will be launched within a 15-year period; the first satellite (ROCSAT-1) is scheduled for launch in October 1997, followed by one launch every 5 years. Under this plan, the ROC's goal is to build a foundation in space science and technology and to develop an autonomous system engineering capability; another objective is to gradually build up ROC's space systems, subsystems and components, to develop system integration techniques, and to actively utilize its space resources.

The 15-year plan will be implemented in two stages; the first stage starts with the initiation of the space development plan and ends when the first satellite becomes operational on orbit (expected to be within 6 years). The main task during this stage is to establish a base structure and develop the basic technologies for space systems. One of the key issues is to emphasize the use of our own resources wherever feasible in building the first satellite; this will include developing the components and subsystems, participating in the design, analysis and construction of payloads (i.e., instruments for scientific experiments), and integration and testing of the satellite and its payload.

The second stage starts from the point when the first satellite becomes operational to the point when the ROC can carry out its space development plan on its own. During this period two small satellites with special space missions will be launched; also, the task of developing the satellite and its payload will primarily be accomplished by domestic industries, government organizations and universities; part of the work will be done by foreign firms in the form of subcontracts.

Achieving the Goal of Complete Self-Reliance

In a satellite development program, comprehensive design plans must be established for both the space segment (i.e., the launch vehicle and the satellite itself) and the ground segment (i.e., the launch system and the telemetry, tracking and command systems). In the 15-year space development plan, our immediate goal is to devote most of our resources to building the ROCSAT-1.

However, because of our lack of experience in building artificial satellites, initially we must rely on foreign aerospace firms to develop the satellite unit itself. Last August, the National Space Program Office (NSPO) started to prepare a "Request for Proposal (RFP) for the Design of the Satellite Unit"; in last December draft copies of the RFP had been sent to interested firms abroad. In May of this year, the finalized RFP will be issued; it is expected that by August, a foreign space system contractor will be chosen to jointly perform the design, development, integration and test of our first satellite—the ROCSAT-1. The final contract will specify that the developer of the satellite module will provide a comprehensive plan for technology transfer and training; through this technology transfer contract, industries in the ROC will be able to build a foundation for developing key technologies such as satellite components and system engineering that will yield long-term economic benefits.

According to the NSPO's spokesman Mr. Wang Ite, the Component Development Department of the NSPO has made an assessment of the capability and interest of domestic industries in producing part of the satellite components. Specifically, 17 domestic companies have been selected to compete for a contract to build 14 components[1] which account for 25 percent of the total hardware costs of ROCSAT-1. Therefore, 25 percent of the satellite components will be provided by ROC in its first satellite; in future development, this percentage is expected to gradually increase until we have the full capability to build the complete satellite module.

Mission Payload Devoted to Scientific Experiments

The primary mission of ROCSAT-1 is to conduct meaningful research in space science; the selection of research topics will be closely coordinated with ROC's existing research capability and ROC's domestic needs. Specifically, the ROCSAT-1 will perform 12 scientific experiments in three different areas:

(A) Exploration of astrophysics: 1) large-scale electrodynamic relationship between the Sun and the Earth; 2) quantitative analysis of plasma dynamics in the low-latitude ionosphere; 3) structure of the low-latitude ionosphere and its interaction with the thermosphere; 4) the effect of solar radiation on the Earth atmosphere; 5) the interaction between the Van Allen Belt and the upper atmosphere.

(B) Remote sensing of the landmass and the ocean: 1) study of the weather system in the tropical and sub-tropical regions; 2) study of water circulation along the coastal regions of different continents; 3) study of the changes in ocean color and temperature and the relationship between water circulation and eddy current.

(C) Experiments in communications technologies: 1) microwave electronic components (receiver/transmitter mixer); 2) solid-state single-crystal microwave integrated circuits; 3) reliability tests of integrated circuits; 4) television broadcast payload.

In addition to its scientific missions, the ROCSAT-1 also performs certain practical functions such as television broadcasting. The candidate scientific instruments to be carried onboard the satellite include a retardation voltage analyzer, a Larmor probe, an ion mass spectrograph, an ultra-violet sun-beam photometer, a high-energy particle spectral analyzer, an ocean color camera and an experimental communications unit.

Cooperation With Mainland China Remains an Option

At the present time, the ROC Government has no plans to develop a satellite launch system; it will primarily rely on other countries to launch the satellite. In fact, NSPO spokesman Mr. Wang Ite indicated that he would not rule out the possibility of using a launch vehicle built by Mainland China if it meets ROC requirements.

During the launch phase and after orbit injection, the status of the satellite is monitored by a telemetry system, its range and velocity are determined by a tracking system, and its operation is controlled by a command and control system. In the 15-year plan, the ground segment—the resource satellite receiving station located at Chungyang (Central) University—will be the first operational segment.

As a result of the technical support provided by Thailand, Australia, Japan, and South Africa, design of the receiving station has proceeded smoothly; a multi-function "Design Requirements" document has been completed, and on-site installation and acceptance testing will begin in April of this year. The station is expected to become operational in June, after which time it will be able to receive and monitor information transmitted by the French SPOT satellite, the European Space Agency's ERS-1 satellite and the U.S. "GOES-6" satellite. Its 13-m antenna can receive signals in the S/X band with a receiving radius of 2,400 km and a data rate of 50 to 100 Mbs (megabits per second); the processing, recording and filing of such an enormous volume of data involves a high degree of advanced information technology.

Completion of the receiving station not only will promote research activities in satellite information technology and in software development and applications, it will also lay a foundation for developing satellite tracking and communication technologies, and for planning our resource satellites.

Developing Ground Segment Subsystems

The primary systems of the ground segment of ROCSAT-1 will be built by foreign contractors; however, it is our intention that the subsystems will be developed by domestic firms. These subsystems include: 1) telemetry, tracking and command station; 2) mission operation network; 3) software and hardware for the control and operating system; 4) flight dynamics facility; and 5) mission operation, maintenance and training facility.

On 13 April of this year, the NSPO invited foreign and domestic firms to a clarification meeting on the "ROCSAT-1 Ground Segment Planning Document"; more than 200 firms attended the meeting (40 percent were foreign firms). The spokesman of NSPO, Mr. Wang Ite, indicated that the purpose of this meeting was to provide an opportunity for domestic companies to make contact with foreign companies in the same industry. The contractual agreement for the ground segment also requires the foreign contractor to provide technology transfer, with the intention of promoting industries in this country. This ground facility will perform the telemetry, tracking and command operations of ROCSAT-1, and collect all the scientific data for analysis by the Research and Development Office.

Basic Organizational Structure and System Integration

Figure 1 shows a diagram of the basic organizational structure of the overall space development effort. The NSPO and its branches share the responsibilities of planning, system engineering, overall quality assurance and administration. The Component Development Center has

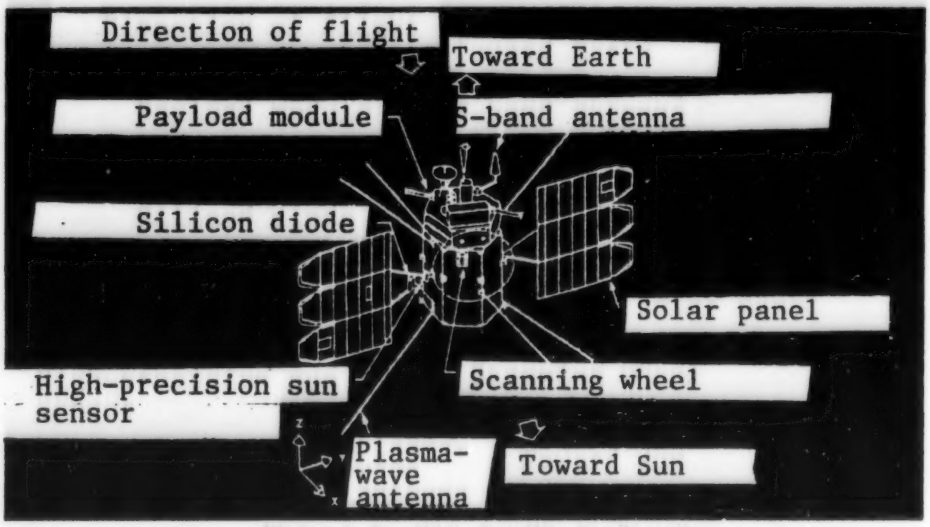

Figure A. Candidate Satellite Configuration

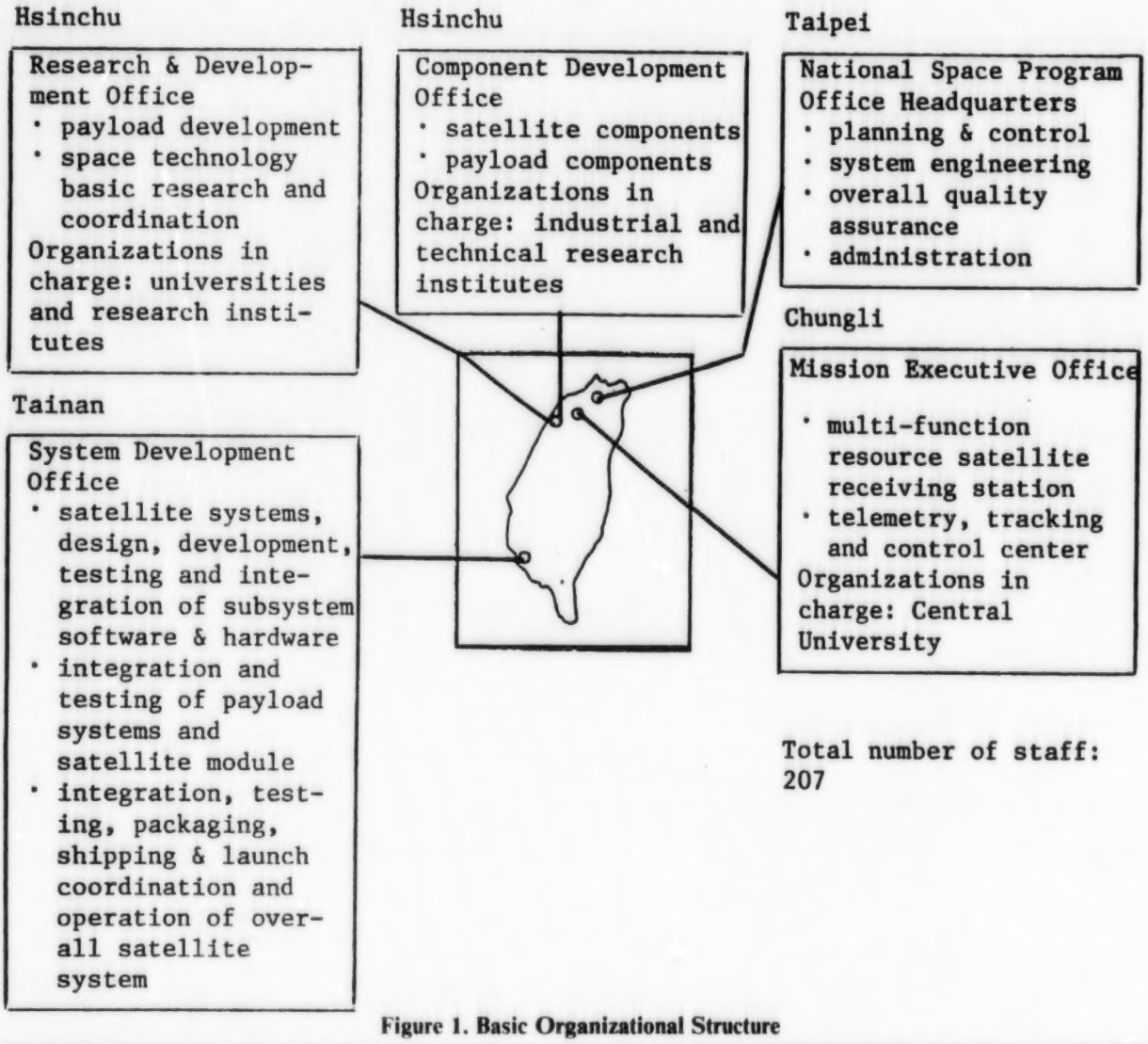

Figure 1. Basic Organizational Structure

the responsibility of developing new components for all three segments of the space system—the satellite, the launch system and the ground station. The Component Development Center and the Mission Operations Office are staffed by both Government and industry personnel. The telemetry, tracking and control center of the Mission Operations Office will be relocated to the Hsinchu Technology Park because the antenna designed for the resource satellite receiving station cannot be used for ROCSAT-1. In addition, a Research and Development Office has also been established; the integration, testing and assembly of the satellite will be carried out in Tainan.

Our Government's main objective in carrying out the 15-year space development plan at such huge expenditure is not only to launch our own artificial satellites and to perform certain missions, but also to promote long-term technological and economic development in this country. Through the space development program, we hope to establish an integrated high-quality, high-tech management system and to encourage active participation from the academic and industrial communities.

Although our space development plan is only targeted for the next 15 years, by the end of this period we should have established a comprehensive structure of the space system and achieved a certain degree of maturity in space engineering and technical experience to meet new challenges and to initiate another long-range development plan.

Footnote

1. The satellite components to be supplied by domestic firms include the following: 1) power converter; 2) solar panel assembly; 3) power regulator, power supply and control unit; 4) antenna; 5) transponder; 6) filter/duplexer; 7) GPS (Global Positioning System) receiver; 8) onboard computer; 9) electronic equipment for attitude and orbit control; 10) solid-state semiconductor recorder; 11) remote terminal interface unit; 12) electric heater; 13) heat pipe; 14) battery.

END OF FICHE DATE FILMED

8 DEC 1993